

Characterisation of Flexible Adhesives for Design

Bruce Duncan and Louise Crocker

Measurement Good Practice Guide No. 45

Characterisation of Flexible Adhesives for Design

Bruce Duncan and Louise Crocker
NPL Materials Centre,
National Physical Laboratory, Teddington.

Abstract:

Flexible adhesives, characterised by low modulus and large extensions to failure, have a long history of use in non-structural applications. However, the advantageous properties of flexible adhesives in sustaining large strains and more evenly distributing peel forces on the bonded substrates are leading to their use for structural joining applications. This is driving the need to improve the understanding of their mechanical properties, which has received little attention, in comparison to structural adhesives. The study of methods for characterising the deformation and failure of flexible adhesives has formed the core of the Flexible Adhesives project of the *Performance of Adhesive Joints* programme supported by the DTI. This Measurement Good Practice Guide describes methods for characterising the hyperelastic and visco-elastic properties required to predict the mechanical performance of a flexible adhesive layer in a bonded structure. The Guide also discusses some aspects of Finite Element modelling of flexible adhesives.

© Crown Copyright 2001
Reproduced by permission of the Controller of HMSO

ISSN 1368-6550

July 2001

National Physical Laboratory
Teddington, Middlesex, UK, TW11 0LW

Acknowledgements

This Guide has been produced in a *Performance of Adhesive Joints* project, part of the *Materials Measurement* programme sponsored by the Engineering Industries Directorate of the Department of Trade and Industry. The advice and guidance from Gareth McGrath (TWI) and the programme Adhesives Industrial Advisory Group are gratefully acknowledged.

The authors would like to acknowledge the contributions of colleagues at NPL – Dr Bill Broughton, Dr Greg Dean, Ms Jeannie Urquhart, Ms Elena Arranz, Mr Keith Ogilvie-Robb, Mr George Hinopoulos and Mr Richard Mera. The assistance of Terry Twine (Risk Statistical Consulting) with the statistical analyses is greatly appreciated.

For further information on *Materials Measurement* contact the Materials Enquiry Point at the National Physical Laboratory:

Tel: 020 8943 6701
Fax: 020 8943 7160
E-mail: materials@npl.co.uk
Website: www.npl.co.uk

Characterisation of Flexible Adhesives for Design

Contents

Executive Summary	1
1. Scope	3
2. Specimen Preparation and Conditioning.....	6
2.1 Bulk Specimen Preparation.....	6
2.1.1 <i>Dispensing Adhesive into a Mould</i>	6
2.1.2 <i>Curing the Adhesive</i>	9
2.2 Assessing Cure State.....	11
3. Tension Test Methods for Flexible Adhesives	13
3.1 Uniaxial Tension Test.....	14
3.1.1 <i>Uniaxial Tension Test Specimen</i>	14
3.1.2 <i>Tensile Strain Measurement</i>	17
3.1.3 <i>Tensile Testing</i>	20
3.2 Planar Tension Test.....	22
3.2.1 <i>Test Specimen and Fixtures</i>	23
3.2.2 <i>Test Procedures</i>	24
3.3 Equibiaxial Tension Test	26
3.3.1 <i>Biaxial Test Equipment and Specimens</i>	27
3.3.2 <i>Strain Measurement</i>	29
3.3.3 <i>Biaxial Tests</i>	29
3.4 Measurements for Modelling Hyperelastic Properties.....	31
4. Methods for Determining Volumetric Properties	33
4.1 Volumetric Compression	34
4.2 Volumetric Tension	36
5. Methods for Determining Visco-Elastic Properties	38
5.1 Stress Relaxation.....	39
5.2 Creep.....	40
5.2.1 <i>Creep Test Apparatus</i>	40
5.2.2 <i>Strain Determination</i>	41
5.2.3 <i>Creep Rupture</i>	42
5.3 Rate and Time Dependent Predictions.....	43

6. Formatting Data For Hyperelastic Materials	45
6.1 Presenting Experimental Data.....	45
6.1.1 <i>Uniaxial, Biaxial and Planar data</i>	45
6.1.2 <i>Volumetric Data</i>	47
6.1.3 <i>Visco-Elastic Data</i>	47
6.2 Calculating Hyperelastic Coefficients.....	48
6.3 Single Element Check.....	50
7. Finite Element Modelling	52
7.1 Comparison of Element Types	52
7.2 Material Models	53
7.3 Mesh Size and Element Type.....	54
8. Failure Criteria	55
9. Concluding Remarks	58
10. Useful Contacts	60
11. References	61
APPENDIX I: Hyperelastic Models	65
APPENDIX II: Example sets of experimental data	70
APPENDIX III: Coefficient calculation input file	73
APPENDIX IV: Single element analysis input file	75
APPENDIX V: ABAQUS Element Types	77

Glossary of Terms

(Based on BSI and ASTM definitions)

Adherend: Body that is, or is intended to be, held to another body by an adhesive.

Adherend failure: Failure of a joint in the body of the adherend.

Adhesion: State in which two surfaces are held together by interfacial bonds.

Adhesive: Non-metallic substance capable of joining materials by surface bonding (adhesion), the bonding possessing adequate internal strength (cohesion).

Adhesive failure: Failure of an adhesive bond such that separation appears to be at the adhesive/adherend interface.

ASTM: American Society for Testing and Materials.

Bond: The union of materials by adhesives.

Bond line: The layer of adhesive that attaches two adherends, also called the bond layer.

Bond strength: The unit of load applied to tension, compression, flexure, peel, impact, cleavage, or shear, required to break an adhesive assembly with failure occurring in or near the plane of the bond.

BSI: British Standards Institute

Butt joint: Joint in which the plane of the bond is at right angles to a major axis of the adherends.

Bulk adhesive: The adhesive unaltered by the adherend.

Cleavage: Mode of application of a force to a joint between rigid adherends, which is not uniform over the whole area, but results in a stress concentrated at one edge.

Cohesion: The ability of the adhesive to resist splitting or rupture.

Cohesive failure: Failure within the body of the adhesive (i.e. not at the interface).

Creep: The time-dependent increase in strain resulting from a sustained load.

Fillet: Portion of an adhesive that bridges the adherends outside the bond line.

Glass transition: Reversible change in an amorphous polymer or in amorphous regions of a partially crystalline polymer from (or to) a viscous or rubbery condition to (or from) a hard and relatively brittle one.

Hyperelastic: Large strain elastic behaviour modelled using a strain energy potential.

ISO: International Standards Organisation.

Lap joint: Joint made by placing one adherend partly over another and bonding together the overlapped portions.

Materials model: Constitutive equations linking stress and strain properties.

Modulus: Material property denoting the stress required to extend a specimen by unit strain. (modulus = σ/ϵ)

Peel: Mode of application of a force to a joint in which one or both of the adherends is flexible and which the stress is concentrated at a boundary.

Poisson's ratio: The ratio between axial and transverse strains in a uniaxial tension test as defined in Equation (3), used in the definitions of elastic moduli.

Post-cure: Further treatment by time and/or temperature of an adhesive to obtain the required properties by curing.

Scarf joint: Joint made by cutting identical angular segments at an angle less than 45° to the major axis of two adherends and bonding the adherends with the cut areas fitted together to be coplanar.

Shear: Mode of application of a force to a joint that acts in the plane of the bond.

Strain: Unit change due to force in size of body relative to its original size (ϵ). Engineering or nominal strain is defined by Equation (2). True strain is defined in Equation (4).

Stress: Force exerted per unit area at a point within a plane (σ)(ϵ). Engineering or nominal stress is defined by Equation (5). True stress is defined in Equation (6).

Stress-strain diagram (or curve): A diagram in which corresponding values of stress and strain are plotted against each other.

Structural bond: Bond that is capable of sustaining, in a structure, a specified strength level under a combination of stresses for a specified time.

Substrate: A material upon which an adhesive is applied.

Surface preparation (or treatment): Physical and/or chemical treatments applied to adherends to render them suitable or more suitable for adhesive bonding.

Tension: Mode of application of a tensile force normal to the plane of a joint between rigid adherends and uniformly distributed over the whole area of the bond line.

Thermoset: A resin that is substantially infusible and insoluble after being cured.

Visco-elastic: A material whose properties combine elastic (or recoverable) and viscous (or irrecoverable) components. Visco-elasticity leads to strain rate and temperature dependent properties and is also responsible for damping.

Yield stress: The stress (either normal or shear) at which a marked increase in deformation occurs without an increase in load.

Characterisation of Flexible Adhesives for Design

Executive Summary

This Measurement Good Practice Guide aims to provide guidance to technologists, laboratory staff and quality assurance personnel on how to characterise and quantify the mechanical properties of flexible adhesives in order to carry out predictive design calculations. Some guidance is given on how to perform Finite Element (FE) modelling of components bonded using flexible adhesives. A general familiarity with laboratory operations and mechanical testing, but not specifically adhesives testing, is assumed. The objective of this Guide is to familiarise the operator with the options available for testing and the factors that can influence the test and design results. It is highly recommended that validation tests be performed to gain confidence in design calculations.

Finite Element Analysis (FEA) is used extensively in the design of structures and sub-components. Accurate predictions of component properties require both suitable material models and accurate material properties data. Highly extensible materials, such as flexible adhesives, cannot be accurately modelled using conventional elastic-plastic material models. These materials require the so-called hyperelastic models. The classical Mooney-Rivlin model is an example of a hyperelastic model that is implemented in FEA packages, such as ABAQUS.

Accurate modelling of hyperelastic materials requires material properties data measured to large strains under different states of stress. In hyperelasticity the strain energy density is modelled as a function of the deviatoric (shear) and volumetric components of the strain tensor. Model coefficients are calculated from mechanical test data using least squares fit routines in the FE software. Methods for obtaining and presenting the required input data are described in this Guide.

The material properties required to calculate deviatoric coefficients can be determined from test data measured under conditions of plane stress (uniaxial tension), plane strain (planar tension) and equibiaxial stress (equibiaxial tension) in order to accurately model the

hyperelastic materials under multi-axial states of stress. These techniques, as developed and applied by NPL, are described further. A common assumption made, particularly for rubbers, is that the material is incompressible, and, thus, volumetric properties can be neglected. However, experimental measurements indicate that flexible adhesives are compressible and that volumetric terms need to be included in the material properties definitions. Test procedures have been developed for determining volumetric properties in tension and compression. The most efficient combination of input test data for performing design predictions using Finite Element methods was found to be uniaxial tension and volumetric tension properties. The provision of data from additional tests had little effect on prediction accuracy but added substantially to the cost and complexity of material characterisation. Time-dependent properties can be characterised through stress relaxation and creep tests.

Hyperelastic test methods require bulk test specimens. Techniques for preparing and curing such specimens are outlined in this Guide. The cure state of the bulk test specimens used to obtain the mechanical properties data should be similar to that of the adhesive in the bonded structure. Cure schedules should be selected to ensure that the thermal histories of the materials are similar in each case. Dynamic Mechanical Thermal Analysis (DMTA) measurements can be made to compare the state of cure of the materials.

1. Scope

The term flexible adhesives is used to describe adhesives and sealing materials whose mechanical responses are characterised by low modulus and large extensions to failure. This Guide is appropriate to thermosetting elastomers, such as polyurethanes and polybutadienes, whose physical properties change irreversibly on cure, and rubber adhesives. The flexibility of the adhesive is strongly rate dependent [1] and these materials can be considered as flexible at or above their glass transition temperature (T_g). Such materials are said to be in the rubber phase. Below T_g , the material is glassy with a much higher stiffness, but reduced extensibility before failure. In comparison with traditional structural adhesives, such as epoxies, little attention has been paid to the mechanical performance and design methods for flexible adhesives. Basic design data for structural adhesives [2], adhesive joint durability [3], adhesive joint testing [4] and modelling structural adhesives [5] are described in other NPL Measurement Good Practice Guides.

The strength of a flexible adhesive joint, as with structural adhesives, is influenced by:

- Surface energies of adhesive and substrate
 - material type
 - surface preparation and contamination
- Wetting of the surfaces by the adhesive to cover the bonded area
 - surface energies
 - flow properties of the adhesive
- The cohesive strength (or ability to resist rupture) of the adhesive
 - the mechanical properties of the adhesive (modulus, yield strength, strain to failure, visco-elasticity);
 - temperature
 - strain rate
 - the failure mode of the adhesive (brittle or ductile).
- Mode of loading and stress distributions

Adhesive joints tend to be designed on the basis of perfect bonding with the assumption that the locus of failure will be in either the adhesive layer or the adherends. Thus, the properties of the interface are ignored in the design. The challenge is to model the continuum behaviour of the adhesive layer in order to predict joint stiffness and strength. Once a crack has formed in the adhesive the remaining behaviour will be dominated by fracture growth. Failure is assumed to originate in regions of the joint where the stress exceeds the cohesion strength of the adhesive. The cohesive strength of the flexible adhesive depends on many factors such as temperature, strain rate and humidity.

Even in simple joint configurations, such as a single-lap shear joint, the resulting stress and strain distributions in the adhesive layer can be extremely complex with a mixture of shear, peel and hydrostatic pressure stresses occurring. Such situations are not easily amenable to closed form analytical methods and it is common design practice to employ Finite Element (FE) methods to predict structural stiffness and stress distributions. In order to accurately predict the performance of the adhesive joint using Finite Element Analysis (FEA) the following information is required:

- Mechanical properties for the adherends and the adhesive
- Dimensions of the parts
- Constraints and loads on the part
- Failure criteria for the materials employed
- Material models for adherends and the adhesive

It is assumed that information on the adherends, joint dimensions, constraints and loading are available and can be modelled accurately. This Guide focuses on continuum material models, test methods for the mechanical properties and failure criteria for the flexible adhesives.

The high extension behaviour of the flexible adhesives can be thought of as analogous to those of rubbers. There is a large body of work on the mechanical performance of rubbers and many material models have been developed to characterise high strain elastic behaviour, known as hyperelastic behaviour [6-20]. Although flexible adhesives tend to be highly filled, and are therefore more complex materials, there is reason to believe that hyperelastic models represent the most realistic of the available material models. Hyperelastic models are

necessary for characterising the large strain, non-linear behaviour of the flexible adhesive. By definition hyperelastic materials are elastic, i.e. deformations are recoverable.

Hyperelastic material models are outlined in Appendix I. All models have the same general formulation [12]. For example the Mooney-Rivlin (or first order polynomial model) is expressed in terms of a strain energy density U :

$$U = C_{10}(I_1 - 3) + C_{01}(I_2 - 3) + \frac{1}{D_1}(J^{\text{el}} - 1)^2 \quad (1)$$

The model can be split in two parts representing the deviatoric strain matrices (I_1 and I_2) and the volumetric elastic strain matrix (J^{el}). The coefficients C_{10} and C_{01} are determined from regression fits to test data measured under various states of tension. The required test data for the hyperelastic models are determined from tests on large bulk test specimens. Methods for preparing such specimens are outlined in Section 2. Suitable tension test methods are discussed in Section 3. Methods for obtaining the volumetric properties of the adhesive are described in Section 4 and methods for time-dependent properties are covered in Section 5. Formatting of test data for input into FEA is discussed in Section 6 and some aspects of FEA are described in Section 7. Section 8 discusses failure criteria.

2. Specimen Preparation and Conditioning

The most accurate method for determining the material properties for use in design calculations is through testing bulk materials rather than joints [2]. The stress distribution in bulk test specimens is known and uniform. There are no contributions to the results from the adherends. Therefore, the measured results yield material properties with minimal manipulation. A further advantage of bulk specimen tests is that large gauge sections allow for more accurate strain measurements [21].

A potential problem with bulk specimen testing is that the material properties of the bulk material may not be the same as those in thin layers in adhesive joints. A study was performed to compare the shear properties of adhesives determined using various bulk and joint specimen tests [22]. This concluded that, for most of the adhesives studied, the differences between the bulk material and the bonded material were insignificant. However, some adhesives did exhibit differences between bulk and bonded materials. This was considered to be due to differences in cure history. It is thought essential that the bulk material sample experiences the same cure conditions, particularly thermal history, as the joint material [23-26].

2.1 Bulk Specimen Preparation

Procedures for preparing samples of bulk adhesive with properties representative of those encountered in thin bond layers have been developed [23] and standardised [24, 25]. This Section describes the application of such methods to flexible adhesives [26].

2.1.1 Dispensing Adhesive into a Mould

All specimen preparation methods should take into account the hazardous nature of the adhesives. COSHH procedures should be followed to minimise operator exposure.

The mould for preparing bulk specimens should be made mostly from metal to ensure good thermal conductivity. Heat needs to flow into the adhesive for heat curing systems and any excess heat generated by the cure reaction should be conducted away in order to maintain a

constant cure temperature as may be experienced by material in the joint. The surfaces in contact with the adhesive should be flat, dry and free from defects. They should be covered with a release coating (e.g. thin PTFE sheet) to facilitate release of the specimen. Frames or spacers are required to control the specimen thickness, 2-3 mm thickness is suitable for many tests [2] although thinner specimens may be more representative of joint layers. Clamps or weights should be used to hold the mould closed whilst the specimen cures.

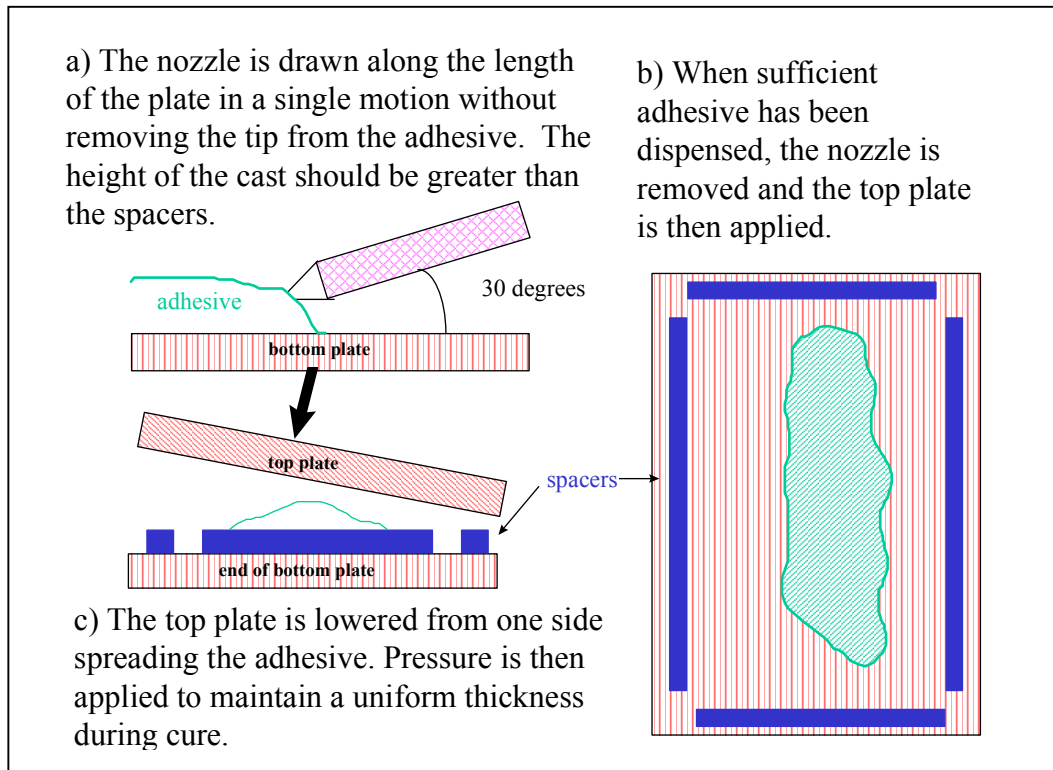


Figure 1: *Dispensing a viscous adhesive to manufacture a plaque of bulk adhesive having a uniform thickness*

Low viscosity adhesives may be dispensed directly into shaped moulds for the production of test specimens. However, many adhesives will not flow readily and such an operation is likely to be ineffective. These adhesives are best produced as flat plaques from which test specimens can be taken after the adhesive is cured.

Care is needed during the dispensing operation to ensure that additional air is not trapped in the final specimen. Procedures such as those shown in Figure 1 can be used, when dispensing through a nozzle, to produce specimens with minimal porosity.

Where possible, two-part adhesives should be mixed by dispensing through static mixing nozzles (either from cartridges or using dispensing equipment). This ensures a uniform mix and a short dispensing time. Hand mixing tends to entrap air into the adhesive. It is essential to maintain a continual flow through the nozzle when dispensing two-part adhesives since interrupted flow may lead to incorrect proportions of adhesive, hardener, etc. entering the nozzle that will cause weak regions in the cast sheet. It should also be noted that the adhesive will start to cure in the nozzle.

High viscosity adhesives can be difficult to dispense into a single ‘cast’ as described above. An alternative method for dispensing these adhesives into the mould is to build up layers of the adhesive by spreading using a specially shaped spatula (Figure 2). A small amount of adhesive is applied at first. This is spread as a thin layer. More adhesive is added gradually and smoothed out along the original layer. The action of spreading the adhesive acts to displace air that may become entrapped in the adhesive. This is a much slower operation for preparing specimens than dispensing directly from a cartridge and, consequently, this method is unsuitable for adhesives with short working lives.

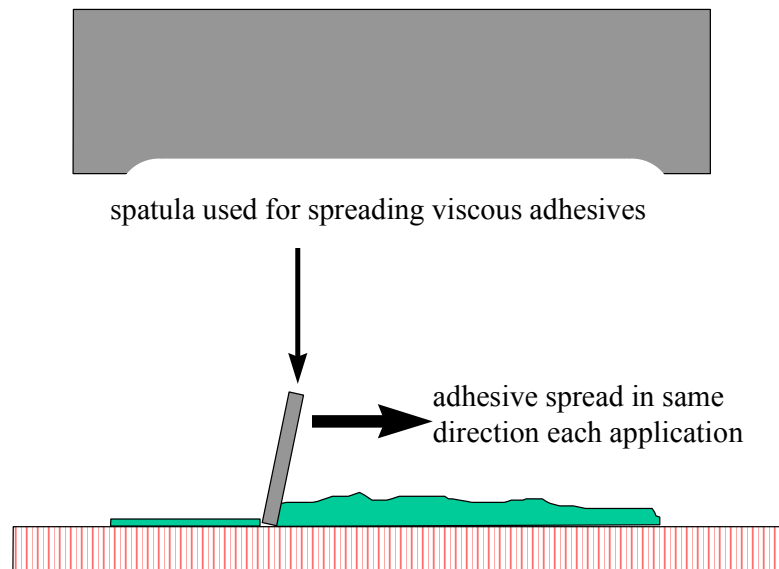


Figure 2: *Bulk specimen manufacture technique for a highly viscous adhesive*

As-supplied adhesive contains varying proportions of entrapped air. Techniques such as vacuum stirring or centrifuging have been suggested as methods for removing air from the adhesive. These techniques have varying degrees of success depending on the viscosity of the

adhesive, but add considerably to the cost of specimen preparation. Plaques can be inspected after manufacture (either visually or by ultrasonic C-scan) to identify regions of low void content from which test specimens can be cut [23].

2.1.2 Curing the Adhesive

Normally, adhesives are cured through cross-linking reactions to solidify the adhesive into a load bearing structure. Cure reactions may be initiated by either chemical means (e.g. 2-part adhesives where resin and hardener are mixed to cure the adhesive) or through energy (e.g. heat or UV activated adhesives). The final cure state and, hence, the mechanical properties of the adhesive will depend on the curing history. Many structural, flexible adhesives are either 2-part or heat cured single-part materials. In order that the material properties of the tensile test specimens are representative of the adhesive layers in the bonded joints it is essential that the bulk material experience the same thermal history during cure as the joint material.

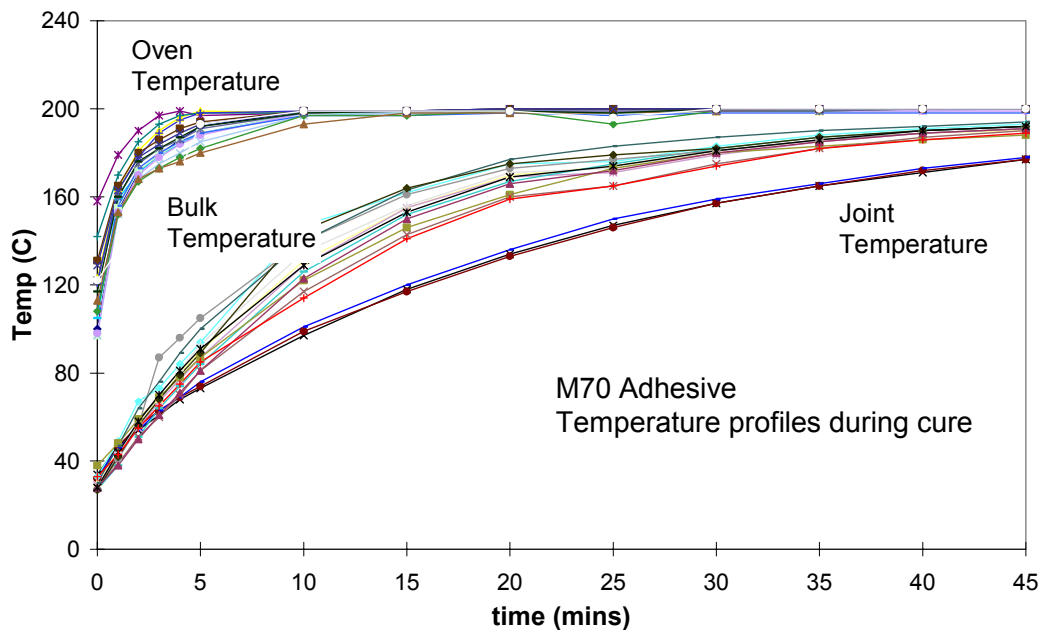


Figure 3: *Thermal histories of bulk and joint specimens cured under identical conditions*

In the case of room temperature curing two-part adhesives, this is done through curing both types of specimen at the same temperature for the same cure time. As time progresses the rate of cure will diminish until an equilibrium structure is obtained in the adhesive. Differences between material properties due to specimen ageing will become less significant as the age of the specimen increases. For example, the differences between specimens cured

for nine weeks and ten weeks will be much less significant than for those cured for nine hours and ten hours.

Bulk adhesive specimens should be cured under conditions that approximate those that occur in the adhesive when the bonded component is cured. There is a danger that the low thermal conductivity of the adhesive may not allow the heat generated by exothermic cure reactions to dissipate. This could lead to excessive temperature rises in the bulk adhesive in comparison to those in the thin layers in joints. Metal moulds should act as heat sinks and prevent excessive temperature rises. However, temperatures in the adhesive during cure should be monitored using a thermocouple embedded in the adhesive in order to confirm the thermal history.

For adhesives cured at elevated temperatures, differences in the effective thermal mass of the bulk specimen mould from the bonded joint may lead to differences in the thermal histories of the adhesives. Simply placing both fixtures into an oven at the same temperature for the same duration does not guarantee equivalent states of cure. Figure 3 shows temperature measurements made whilst curing bulk adhesive specimens and adhesively bonded lap joint specimens. The temperature of the specimens lags that of the oven. The joint specimens are slower to heat than the bulk test specimens. The final temperature of the adhesive in the joint at the end of the cure period is significantly lower than in the bulk adhesive.

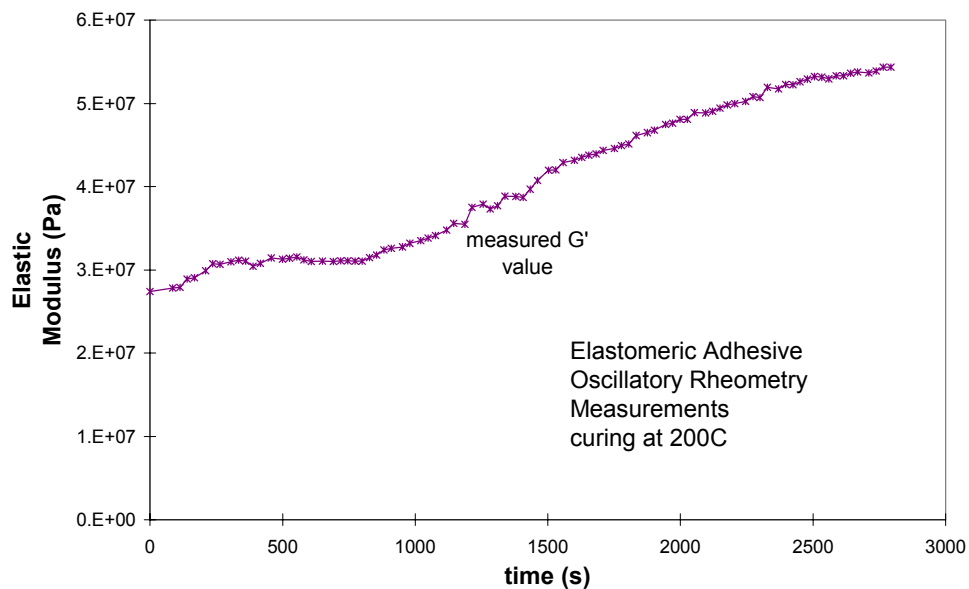


Figure 4: Development of modulus during cure

Development of adhesive structural properties during cure can be studied directly from the increase of the material modulus (Figure 4). This can be measured by either oscillatory shear rheometry or ultrasonic methods [27, 28]. Such studies enable the establishment of optimised cure schedules. However, equally important is information on how rapidly the bonding fixture heats. With this information the cure schedules for the bulk specimens can be adjusted to give comparable thermal histories and, therefore, representative test specimens can be produced. In the example shown in Figure 3, it was found that increasing the oven temperature by 15 °C when curing joint specimens gave material with mechanical properties comparable to the bulk specimens.

2.2 Assessing Cure State

The cure states of adhesive specimens may be compared using measurements of the glass transition temperatures (T_g) of the specimens. T_g marks the transition between a rigid glass-like structure and a flexible rubbery structure. Many material properties, for example thermal expansion coefficients, thermal conductivity, elastic modulus, will show non-linear discontinuities around T_g and these can be used to determine T_g . The most convenient means are through thermal (Differential Scanning Calorimetry, DSC) or mechanical (Dynamic Mechanical Thermal Analysis, DMTA) methods [29]. Although it is possible to correlate T_g values determined from different test methods it is recommended that samples be compared using the same test method [29].

DMTA probes the mechanical properties but requires sizeable samples that are typically at least 20 mm long. Samples can be cured in most joint configurations and, by use of low surface energy coatings on the adherends, released after cure. DSC requires samples weighing fractions of a gram. Thus specimens are smaller and, therefore, easier to obtain.

The Dynamic Mechanical Thermal Analysis (DMTA) data in Figure 5 show that the differences between thermal histories evident in Figure 3 lead to differences between the mechanical properties. T_g is determined from the temperature of the peak in the viscous modulus curve (E''). Since the objective of testing the bulk specimens is to determine material properties for use in designing joints, differences between the material properties will lead to inaccuracies in the design predictions.

Whilst specimen preparation is key to producing representative test specimens, the storage of the sample between manufacture and testing can have significant influence on the material properties. For example, adhesives that cure at room temperature often continue to cure for a significant period of time after cure is nominally ‘complete’. These specimens should either be post-cured or stored at low temperatures to reduce the variability in results due to specimen age. If required, curve-fitting routines can be used to determine the location of the peak [29]. The moisture content of the adhesive will affect its mechanical properties. Therefore, post-manufacture moisture adsorption by the specimens is another factor to consider.

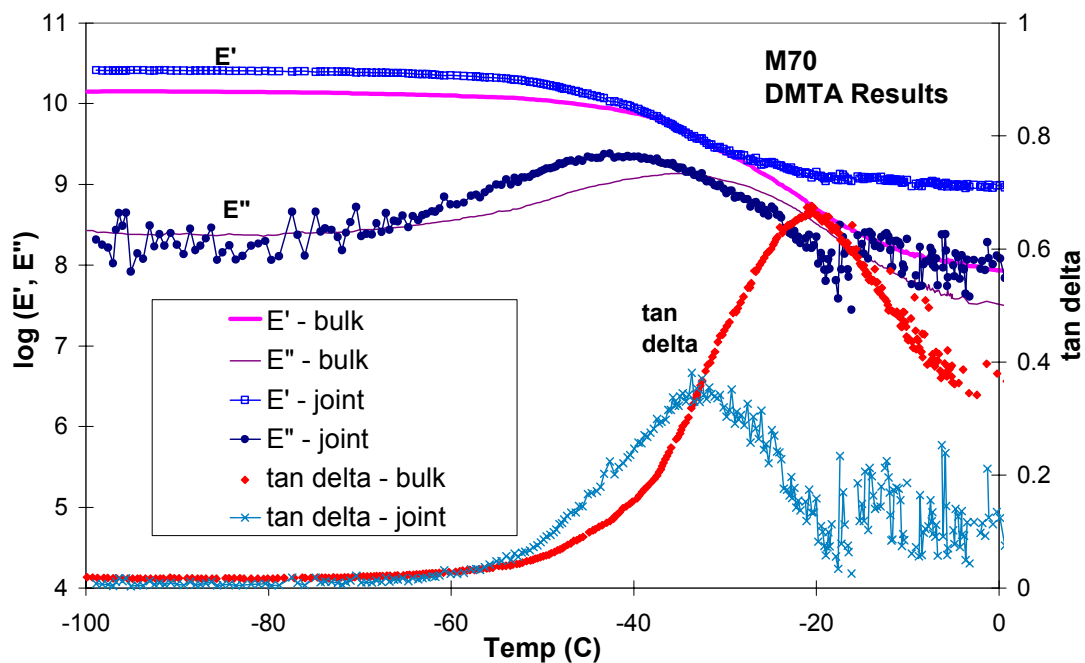


Figure 5: *DMTA results showing the properties of adhesive cured in the bulk specimen and joint specimen preparation fixtures*

3. Tension Test Methods for Flexible Adhesives

Finite Element manuals [12, 30] suggest that the most accurate representation of the hyperelastic properties of the adhesive will be gained if the input coefficients are determined from a combination of:

- Uniaxial Tension (Section 3.1)
- Plane Strain or Planar Tension (Section 3.2)
- Equibiaxial Tension (Section 3.3)

Flexible adhesives are visco-elastic materials, i.e. their mechanical properties will depend on strain rate and temperature [1, 31]. As shown in Figure 6, relatively small changes in test or service condition can have dramatic consequences for mechanical properties. The sensitivity of low strain properties to temperature and frequency can be rapidly established using dynamic test techniques such as DMTA or oscillatory shear rheometry. However, such techniques are limited to low strain behaviour and cannot provide the accurate large strain behaviour needed for design [32]. This section discusses large strain mechanical measurements in tension [19, 33, 34].

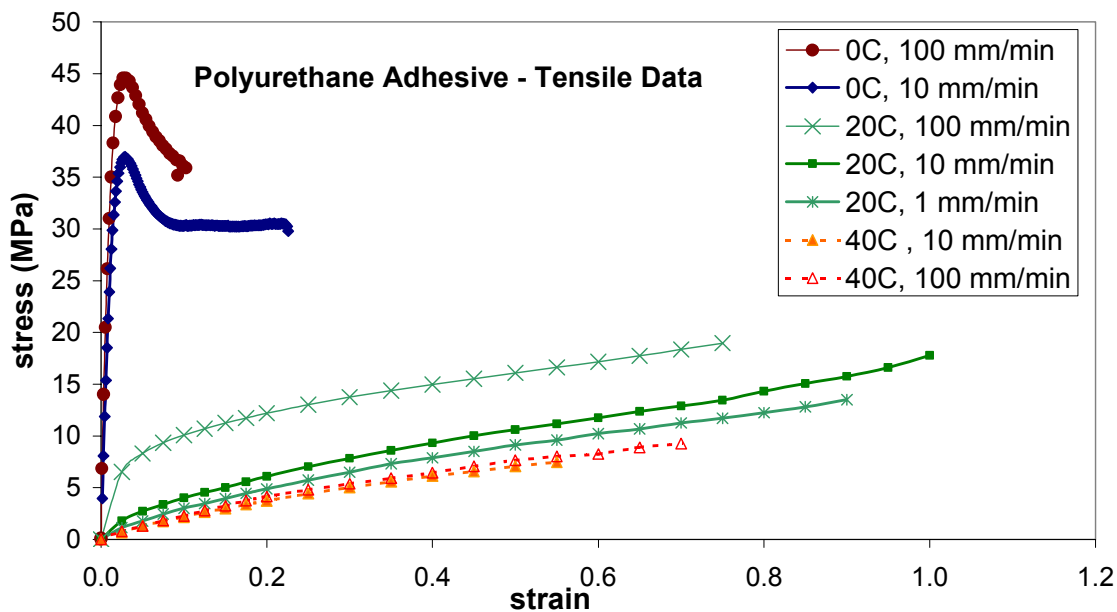


Figure 6: Tensile properties of polyurethane adhesive

It is essential that materials properties are determined under test conditions appropriate for the service conditions in order for the design predictions to be relevant. Where combinations of test data are supplied to derive model coefficients, these data must be determined at the same temperatures and strain rates. Test speeds will need to be selected in order to achieve comparable rates of strain in the different test specimens. It is essential that test times are available from the test data in order that actual strain rates in the specimen can be determined. Some testing machines have data reduction or data compression routines to reduce the number of points recorded during testing. These functions can cause problems with determination of time in the test. Unless time is directly recorded or the data reduction algorithms are periodic and well understood it is recommended that these functions be disabled when performing tests.

3.1 Uniaxial Tension Test

The uniaxial tension test determines the properties of the material under plane stress. Various standard tension test methods are specified for plastics [35, 36] and rubbers [37, 38]. The main differences between the plastics methods and the rubber methods arise from the test specimen geometry and loading speeds. As noted above, the test speed needs to be selected in order to apply strain at a rate representative of the service performance requirements. Therefore, selected rates are likely to deviate from both types of standard. The test specimens are discussed in Section 3.1.1. The standard rubbers test methods [37, 38] also allow for the testing of ring specimens, but these are unsuitable for flexible adhesives owing to difficulties in specimen preparation.

3.1.1 Uniaxial Tension Test Specimen

Tension tests are performed on dog-bone shaped test specimens, see Figures 7 and 8 and Tables 1 and 2. This arrangement provides for a uniform stress and strain distribution in the central gauge section, where these values are at a maximum. Thus, the specimen extends and fails under well-defined conditions. Flexible adhesives will sustain large extensions prior to failure. This will place limitations on the geometry of the test specimen to fail specimens within the travel of the test machine.

The ISO 3167 multi-purpose test specimen [39] with a minimum length of 150 mm and a gauge width to gripped width ratio of 1:2 is recommended for structural adhesives [2]. However, this is probably too large for flexible adhesives. A smaller test specimen may be more appropriate and the plastics tensile standard [35] allows for a half-sized test-piece (Figure 7). The rubber test standards specify a sample with a smaller gauge width to gripped width ratio (Figure 8). Dimensions for standard plastic and rubber test specimens are shown in Tables 1 and 2, respectively. There is no preference as to which type of specimen is tested but it should be noted that test results obtained from different geometries might not be identical. All tensile properties discussed in this Guide were obtained from Table 1, Type 1BA specimens.

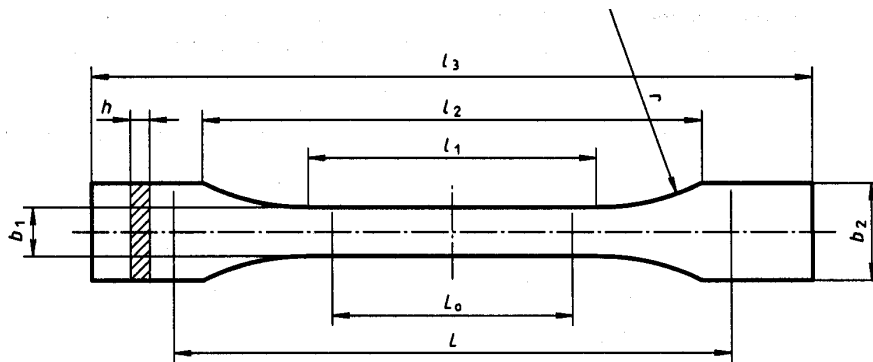


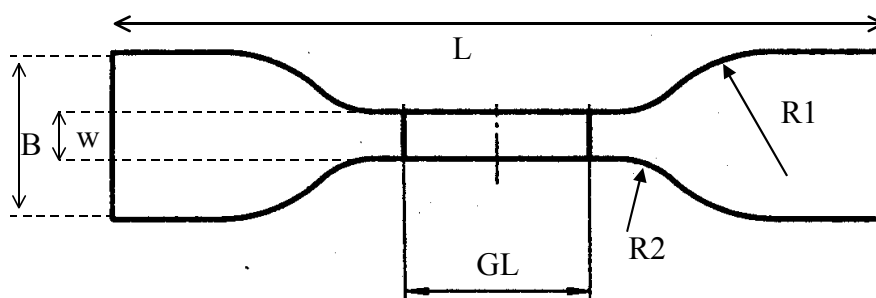
Figure 7: ISO 3167 or ISO 527-2 plastics test-piece

Table 1: Dimensions (in mm) of ISO 527 test specimens for plastics (Figure 7)

	Dimension	Type 1A	Type 1B	Type 1BA	Type 1BB
l_1	Length of narrow parallel-sided portion	80 ± 2	80 ± 2	30 ± 0.5	12 ± 0.5
l_2	Distance between broad parallel-sided portions	104-113	106-120	58 ± 2	23 ± 2
l_3	Overall length	≥ 150	≥ 150	≥ 75	≥ 75
r	Shoulder radius	20 - 25	≥ 60	≥ 30	≥ 12
b_1	Width of narrow portion	10 ± 0.2	10 ± 0.2	5 ± 0.5	2 ± 0.2
b_2	Width at ends	20 ± 0.2	20 ± 0.2	10 ± 0.5	4 ± 0.2
h	Preferred thickness	4.0 ± 0.2	4.0 ± 0.2	≥ 2	≥ 2
L_0	Preferred gauge length	50 ± 0.5	50 ± 0.5	25 ± 0.5	10 ± 0.2
L	Initial distance between grips	115 ± 1	$l_2 + 5$	$l_2 + 2$	$l_2 + 1$

Table 2: Dimensions (in mm) of ISO 37 test specimens for rubbers (Figure 8)

	Dimension	Type 1	Type 2	Type 3	Type 4
L	Minimum total length	115	75	50	35
GL	Length of gauge section	33.0 ± 2.0	25 ± 1.0	16.0 ± 1.0	12.0 ± 0.5
B	Width of ends	25.0 ± 1.0	12.5 ± 1.0	8.5 ± 0.5	6.0 ± 0.5
W	Width of gauge section	6.0 ± 0.4	4.0 ± 0.1	4.0 ± 0.1	2.0 ± 0.1
R1	Transition radius (inner)	14.0 ± 1.0	8.0 ± 0.5	7.5 ± 0.5	3.0 ± 0.1
R2	Transition radius (outer)	25.0 ± 2.0	12.5 ± 1.0	10.0 ± 0.5	3.0 ± 0.1

**Figure 8:** ISO 37 test-piece

These specimens can be moulded directly provided that a suitable mould is available and the adhesive flows sufficiently well to fill the mould. The specimens can also be cut from sheets of bulk material. Owing to their low stiffness, flexible adhesives can be difficult to machine using milling equipment. Specimens can be cut using a sharp scalpel blade and a shaped former, but care must be taken to avoid nicking the edge of the specimens. Shaped cutters mounted on punches provide the most efficient means of producing the uniaxial tension test specimens.

3.1.2 Tensile Strain Measurement

Strains are the normalised extensions in the test sample. They are normally determined from the relative movement of two gauge marks separated by a known distance. Strains can be measured in any direction, but in the uniaxial tension test it is normal to determine the axial strain in the direction of the specimen and machine axis and the transverse contraction strains perpendicular to the machine axis across the width of the specimen. The nominal or engineering strains in each direction are calculated using the following expression:

$$\varepsilon = \frac{d - d_0}{d_0} \quad (2)$$

where, ε is the strain at time t , d_0 is the initial distance between the gauge-lines ($t=0$) and d is the distance between the gauge lines at time t . The axial strain is used in the determination of the modulus and stress-strain curves required as input for the FE analyses. The ratio of transverse strain (ε_t) to axial strain (ε_a) is used to calculate Poisson's ratio ν .

$$\nu = -\frac{\varepsilon_t}{\varepsilon_a} \quad (3)$$

True strains (ε_T), including the effects of incremental increase in gauge length are defined from the nominal strains (ε)

$$\varepsilon_T = \ln(1 + \varepsilon) \quad (4)$$

The low stiffness and large strain to failure of rubbery flexible adhesives prohibit the use of contacting strain measurement devices, such as strain gauges or clip-on knife-edged displacement transducers [21]. Non-contacting strain measurement methods are necessary. Video extensometry or measurement of grip movements are commonly used non-contacting measurement methods.

Strains can be calculated through analysis of the positions of contrasting gauge marks on the surface of the test specimens. These can be recorded in photographs or video recordings made during the test. From the analysed mark separations the strain can be determined. This is the basis of video extensometry where real-time determination of extensions occurs. If no video extensometer is available then a series of photographs made at known loads can be used to determine stress-strain curves from uniaxial tension tests. Gauge extensions can be determined through visual examination of photographs using an appropriate graticule or using

various image analysis software packages commonly available for the computer. However, off-line image analysis is, time-wise, an inefficient approach.

Video extensometers automate the analysis of images and calculate real-time strains during the tests. Video extensometers are a valuable tool for the characterisation of highly extensible materials, which have been used successfully to determine strains, particularly at high extensions, in tension tests [21]. Several test equipment manufacturers supply such equipment. Video extensometers are extremely flexible with regard to strain measurement ranges. Since the strain determination is from an image, with the appropriate zoom lens, wide ranges of gauge sections can be measured. The camera can zoom in to a small region for more accurate, low strain measurements or zoom out to follow larger extensions. Since the measurement device is remote from the sample strain measurement should be unaffected by the specimen environment (for example by looking through a window into an environmental chamber strain measurements can be made at extreme temperatures).

In the Flexible Adhesives project, strain measurements were made using a non-contacting Messphysik ME64 video-extensometer. In this instrument, images in the field of view of the camera are analysed to locate the positions of contrasting gauge marks on the specimen surface. The changes of gauge mark positions relative to their starting positions are used to determine strains. This device has the capability of measuring extensions simultaneously in two orthogonal directions. This is particularly useful for the simultaneous determination of the axial extension and transverse contraction in a uniaxial test specimen to determine Poisson's ratio and, as outlined in Section 4, input data to model volumetric properties.

Accurate strain measurements using video extensometry require a stable, sharp, high-contrast image of the test specimen. The gauge marks should give good contrast against the specimen surface.

The specimen should be well lit. Where no environmental chamber is used on the test machine then the specimen can be lit using spotlights. However, the light intensity and arrangement should be selected such that the lights do not heat the specimen. If an environmental chamber is used then this should have a sufficiently sized window for viewing the specimen gauge section. The sample can be lit using lights inside the chamber, but it is

generally preferable to light from outside of the chamber to avoid heating the specimen. The sample can be lit through the chamber window although spotlights tend to be reflected off the glass. A better solution is to mount more diffuse strip lighting by the chamber window. The lights used should not flicker as this may be interpreted as strain.

The camera should be stable. Cameras for video extensometry should be mounted securely to avoid camera shake that can effect strain measurement. Cameras may be mounted on tripod stands, although this will take up quite a lot of floor space and impede access to the test machine. It is preferable to mount the camera on the test machine using a bracket. Where environmental chambers are used, a mounting bracket containing a light source is recommended.

High contrast gauge marks are required. Normally axial gauge marks are applied perpendicular to the axis of the specimen, using a marker pen in a colour (normally black or white) that gives a high contrast to the specimen surface. It is important that the ink wets the specimen surface, forms a uniform layer and does not degrade at large strains. Highly reflective (e.g. silver) markers can also give high contrast in the correct lighting. A further method is to attach contrasting marks (e.g. self adhesive labels or tapes) to the specimen surface. Attached marks enable high contrast, for example by printing a black line on a white label, with neutrally coloured or grey specimens. The attached marking system is also insensitive to colour changes of the specimen, e.g. stress whitening, or thinning of the marks during extension. However, it is vital that the marks do not move during extension. Such marking strategies can be also used to measure transverse contractions. Provided that the video extensometer is square to the surface of the specimen so that the edges are not visible then the sides of the narrow parallel section of the specimen can be used as gauge marks. Contrast can be maximised through placing black or white card behind the specimen.

Values for axial extensions can be estimated from the movement of the grips [40]. The grip extension should equal the crosshead displacement since the flexible adhesive specimens have low stiffness in comparison to the test machine and extension of the load train should be insignificant. Crosshead displacement can be determined directly from displacement transducers that are commonly part of the machine control system (or from the test time and known constant test speed, but this method is even less accurate). An axial strain value can

then be derived from the ratio of this displacement to initial grip separation. This value will differ from the actual strain in the centre of the specimen since the strain distribution in the specimen is not uniform and strains are further distorted due to gripping effects. It is possible to correlate strains determined through crosshead extension measurements with those measured locally through the concept of an effective gauge length [40]. Regression fits of plots of measured local strain against crosshead extension can be used to calculate an effective gauge length, although the relationship between extension and strain could be non-linear. This effective gauge length could also depend on factors such as specimen geometry, test machine and grip compliance, specimen stiffness and specimen extension. With a rigid, well-clamped load train and a low stiffness flexible adhesive specimen it is probable that there is a reasonable linear relationship between local strain and crosshead displacement that will produce an effective gauge length that is not overly sensitive to specimen geometry or stiffness. Such correlations can be derived using either video extensometry or photographic methods.

3.1.3 Tensile Testing

In all tests, the specimen should be allowed to equilibrate at the test temperature for a sufficient period to ensure a uniform specimen temperature. Generally, the greater the difference between storage and test temperatures the longer the equilibration period, but it should be noted that exposure to elevated temperatures may lead to additional cure or thermal ageing of the specimen. The sample should not be tightly clamped in the grips while the temperature changes as thermal expansion/contraction could over stress the specimen.

Tests should be conducted, at constant rates of extension, using a tensile test frame fitted with a low capacity load cell so that sufficient measurement resolution can be obtained. It is recommended that a computerised data acquisition system be used to record the test time, load cell, extensometer and the crosshead displacement outputs. Nominal or engineering stress is calculated from the load values obtained from the load cell and the un-deformed cross-section using the following equation:

$$\sigma = \frac{F}{w_0 t_0} \quad (5)$$

where, σ is the stress, F is the applied load; w_0 and t_0 are the initial width and thickness of the specimen, respectively. The strain is determined using Equation (2). The true stress can be calculated from the nominal stress and the deformed cross-section area:

$$\sigma_t = \frac{F}{wt} = \frac{F}{w_0(1-\varepsilon_t)t_0(1-\varepsilon_t)} = \frac{\sigma}{(1-\varepsilon_t)^2} \quad (6)$$

where w and t are the deformed width and thickness respectively, ε_t is the transverse contraction strain (assumed to be the same in the width and thickness directions to simplify data determination).

Initial low strain tests (limited to 5 % strain or less) should be performed to determine the strain rate in the specimen during the test. The test strain should be determined from the slope of the strain-time plot and the test speed adjusted to achieve the desired strain rate. Once the test speed required to achieve the desired strain rate has been determined then the test specimen should be allowed to recover for a period at least ten times longer than it was loaded before further testing. The test should be run until the specimen fails. Typical stress-strain behaviour are shown in Figure 9.

It is most likely that flexible adhesives will exhibit behaviour type (c) in Figure 9 although both types (a) and (b) are possible. The tensile strength is defined as the maximum stress sustained by the specimen whether that is at break or yield.

It is recommended that a minimum of five specimens be tested in order to examine repeatability of measurements. If the results are scattered then the stress-strain curve required for determining hyperelastic properties can be obtained either by selecting a representative curve (with the option of choosing extreme curves to investigate sensitivity to material variability) or by averaging the measured curves (one method of doing this is to extract stress values at defined strains from each curve and average these stress values at each strain to produce an ‘average’ curve). Data are formatted for FEA as nominal stress and nominal strain values as described in Section 6.

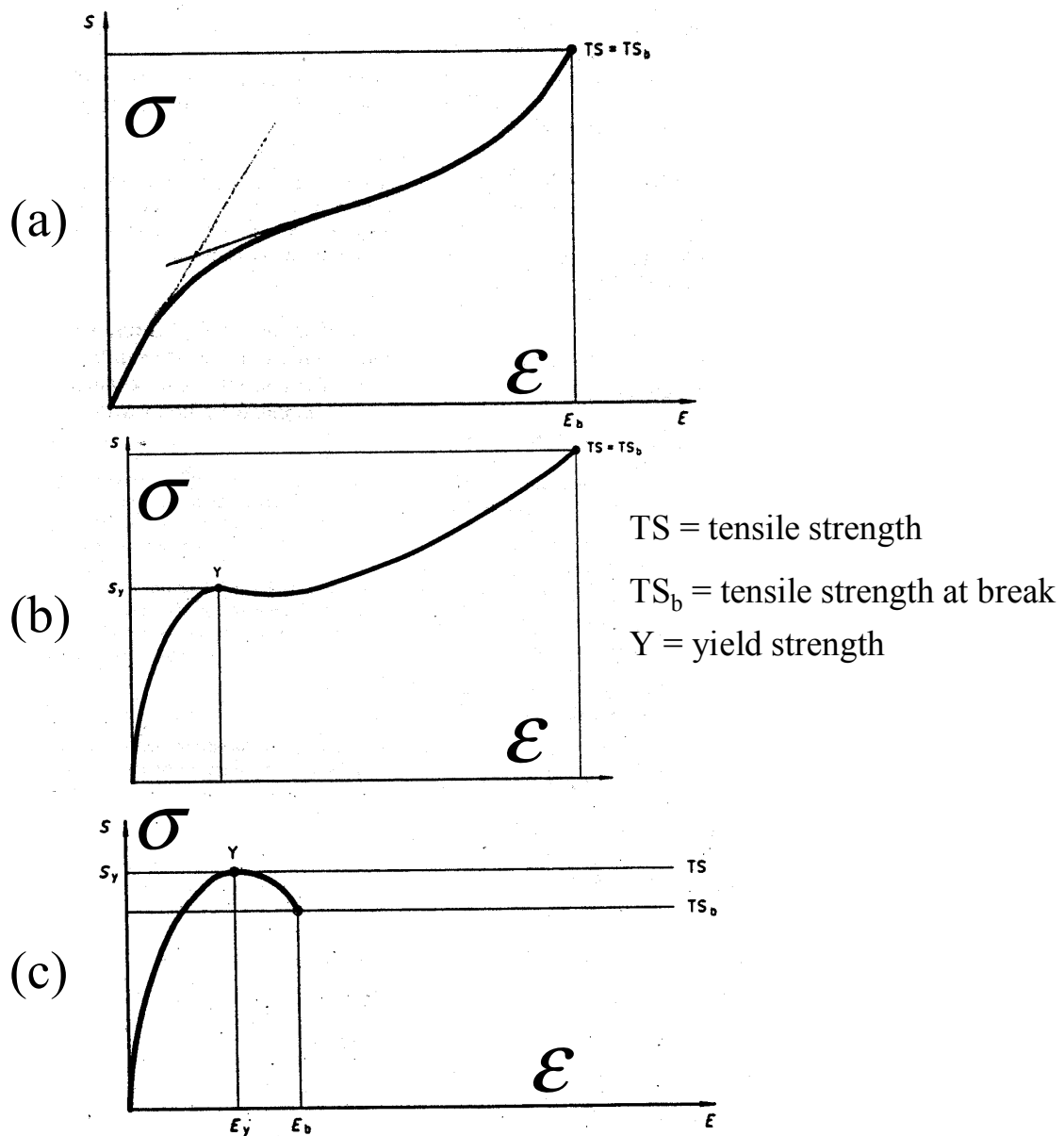


Figure 9: Typical tensile test stress-strain curves for rubbers

3.2 Planar Tension Test

Planar tension test specimens have large aspect ratios (ratio of width to gauge length). If the material is incompressible, then the principal stretches λ_i along the $i = 1, 2, 3$ axes (corresponding to length, width and thickness respectively) are: $\lambda_1 = \lambda_s$, $\lambda_2 = 1$ and $\lambda_3 = 1/\lambda_s$ where λ_s is the stretch in the loading direction (and the nominal strain in the loading direction $\epsilon_s = \lambda_s - 1$). The ABAQUS manual [12] claims that this test is a ‘pure shear test’ since, in terms of the logarithmic strains: $\epsilon_1 = \ln \lambda_1 = -\ln \lambda_3 = -\epsilon_3$ and $\epsilon_2 = -\ln \lambda_2 = 0$, which

corresponds to a state of pure shear at 45° to the loading direction. However, this ‘pure shear state’ may not occur with flexible adhesives since most flexible adhesives are slightly compressible.

3.2.1 Test Specimen and Fixtures

The key feature of the planar test is that, unlike conventional uniaxial tensile tests, there are no lateral strains. Experimentally this is achieved by using specimens with an extremely high aspect ratio (Figure 10). A minimum ratio of width to gauge length (grip separation) of four is recommended. Experimental studies [33] on 200 mm wide x 60 mm long test specimens gripped at different lengths have shown that stress-strain curves are unaffected by aspect ratios between four and ten (Figure 11). A free length of 40 mm, giving an aspect ratio of five, was chosen as a suitable test gauge length. Thus, the specimen is tested in a condition of plane strain rather than the plane stress state that characterises the uniaxial tension test.

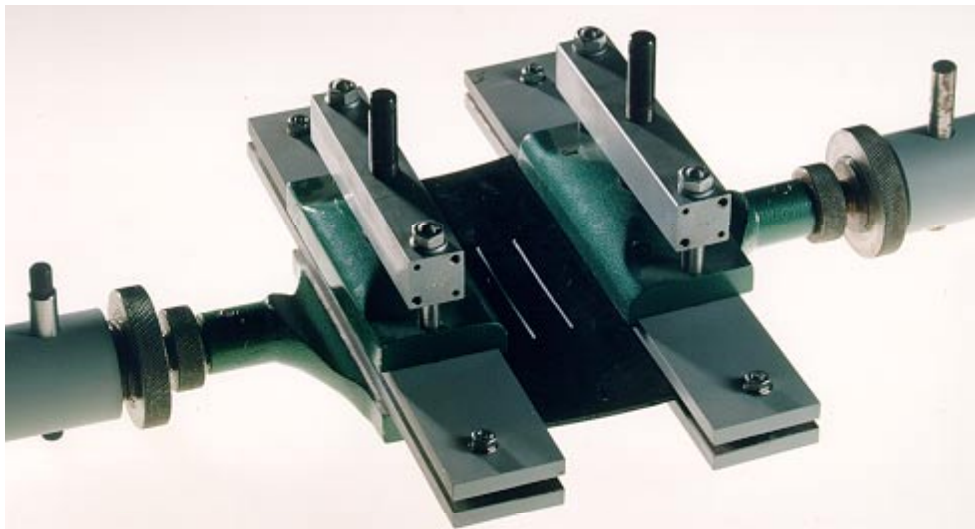


Figure 10: *Planar tension specimen and grips*

In order to test the flexible adhesives under plane strain conditions lateral contraction of the specimen during extension must be minimised. This is normally achieved by testing short, wide specimens. A typical test arrangement and suitable grips, with 300 mm wide jaws, are shown in Figure 10. For reliable planar test results, it is essential that the specimen be firmly gripped so that the specimen does not slip. The grips have to constrain contraction along the whole width of the specimen. The jaws shown in Figure 10 can be tightened at the centre and at each end in order to distribute clamping pressure over the whole width of the specimen. To

ensure the specimens were securely held in the grips and improve the uniformity of clamping four additional clamping bolts were later added to the apparatus shown in Figure 10. It is also possible to reduce the likelihood of the specimen slipping by bonding rigid strips (e.g. 1 mm thick aluminium) to the top and bottom edges of the specimen using a high strength anaerobic adhesive. The adhesive used to attach the strips must not degrade the test sample. This arrangement allows uniform distribution of force on the sample even if the clamping pressure is not equally distributed.

The adhesive test specimen is obtained from bulk sheets manufactured using the techniques outlined in Section 2. Specimens are cut to shape using a shaped template and a sharp scalpel blade. Care must be taken to avoid nicking the edges of the test specimen. The test is more tolerant of damage to the edges in the gripped regions than it is to damage to the free edges. If there are nicks on the free edges the specimens should be discarded.

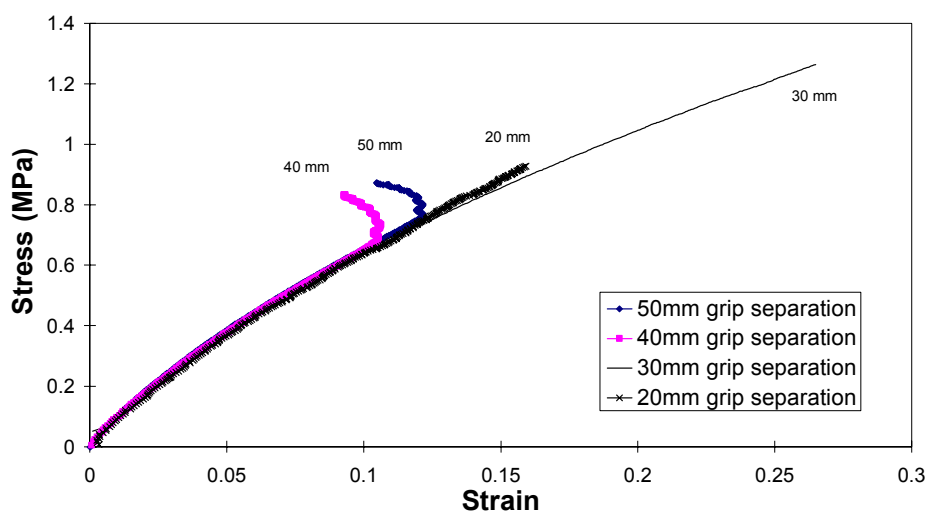


Figure 11: *Evaluation of the effect of aspect ratio on planar tension results*

3.2.2 Test Procedures

The planar tension test is performed in a universal testing machine. The specimen should be conditioned at the test temperature before it is clamped in the grips. The specimen is pulled in tension at a constant extension speed, selected to give a strain rate in the sample that is appropriate for the design analysis. It is recommended that preliminary tests be performed, at low extensions, to determine the relationship between extension speed and strain rate. The

planar stress (σ_p) is straightforward to calculate from the measured force (F_p) and the specimen width (w) and thickness (t):

$$\sigma_p = \frac{F_p}{wt} \quad (7)$$

Strains are more complicated to determine. It is recommended that video extensometry is used to determine strains directly from the movement of contrasting gauge marks on the specimen surfaces. If video extensometry is not available then it is preferable to estimate strains from measured movements of the test grips rather than the crosshead movement. An area of concern was that the planar test specimen might not necessarily experience pure plane strain during testing. Experimental measurements were made to confirm plane strain conditions. Video extensometry was used to show that lateral contractions in the specimen width are minimal and that the axial strain distribution is uniform across the width of the specimen [32].

Termination of the test normally occurs due to two reasons.

- The first cause for ending the test is that the specimen starts slipping in the grips. This is accompanied by a reduction in load or a saw tooth pattern if there is a slip-stick occurrence. The chances of this happening can be minimised by altering the clamping to produce a uniform clamping pressure. Contractions in the thickness of the specimen will occur under extension and, thus the clamping pressure will reduce throughout the test. Wedge or pneumatic grips would help maintain the clamping pressure throughout the test but are not readily available with the appropriate widths.
- The second cause of test termination is failure of the specimen. There are large stress concentrations at the corners of the specimen. Rupture of the specimen originating at the corners can lead to the specimen tearing along the grips. It is thought that the initiation of rupture will have some dependence on the clamping pressure and the sharpness of the grip edge. The jaw faces indent the soft sample when they are tightened. This increases the local stress on the specimen and, if the edge of the jaw is sharp, may 'cut into' the material producing a 'notch'. The obvious solution is to reduce clamping forces but this increases the risk of the sample slipping. Tapping the specimen helps to reduce this notching effect. Adhesive tape (e.g. electrical insulating tape) can be applied to the long edges of the specimen. The indentation of the jaws is thus 'blunted' and the specimen should reach greater loads before tearing.

Any tests carried out on the planar test specimen have tended to fail at strains that are less than 50 % of the strains achieved in the corresponding uniaxial tension test. The cause of failure was either the specimen slipping from the grips or specimens tearing at the corners. Test specimen preparation is time consuming, as a large volume of adhesive has to be dispensed and formed into a uniformly thick sheet that is free of major flaws. In practice, it is difficult to make bulk sheets of sufficient quality to test. This test method is not easily applicable to flexible adhesives.

Test data are formatted for FEA as nominal stress, nominal strain as described in Section 6.

3.3 Equibiaxial Tension Test

Biaxial tension is produced through deforming a specimen simultaneously in two directions. Equibiaxial tension tests require a stress state with equal tensile stresses along two orthogonal directions. Assuming incompressibility, this deformation mode is characterised in terms of the principal stretches: $\lambda_1 = \lambda_2 = \lambda_b$ and $\lambda_3 = 1/\lambda_b^2$ where λ_b is the stretch in the perpendicular loading directions. The nominal strain is defined by $\epsilon_b = \lambda_b - 1$.

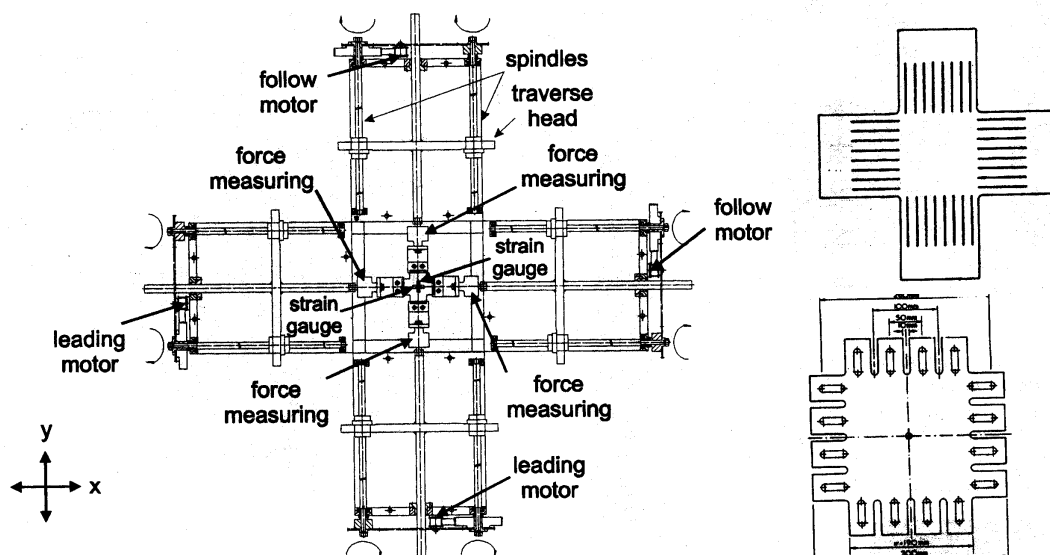


Figure 12: Biaxial testing machine and specimens

3.3.1 Biaxial Test Equipment and Specimens

The equibiaxial stress state is obtained by stretching a square sheet in a biaxial test machine. Mechanical testing machines with two independently moving loading axes are rare in test laboratories owing to their size and expense. Schematics of a typical biaxial test arrangement and cruciform test specimens [41] are shown in Figure 12. The cruciform specimens required for biaxial testing in this type of equipment are relatively large (the specimen arms are approximately 200 mm long) and so may present problems for specimen manufacture.

The scale and expense of this testing was thought unsuitable for flexible adhesives or similar materials and a test fixture has been developed to enable the performance of equibiaxial tension measurements in uniaxial test machines (Figure 13).

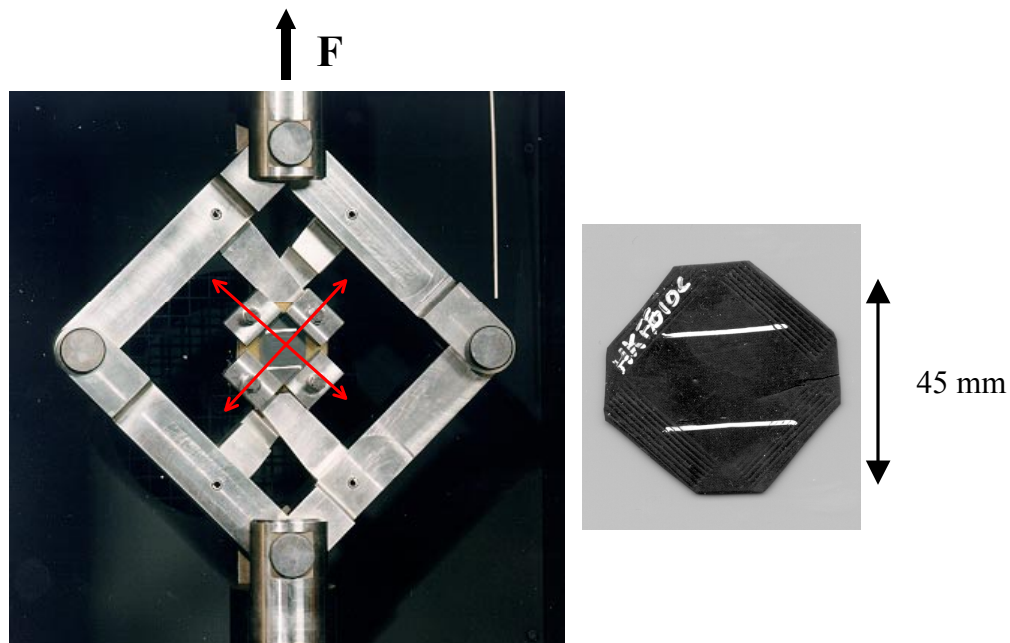


Figure 13: *NPL Biaxial test frame and specimen*

This test fixture consists of pivoted scissor arms that resolve the machine crosshead movement into extension of the test specimen at $\pm 45^\circ$ to the axis of the test machine. As the frame is extended the outer pivots move inwards, applying forces to the inner arms that pull the inner grips apart symmetrically in orthogonal directions. The specimen is extended in local axes at $\pm 45^\circ$ to the axis of the test machine. The total force measured on the pull rod of the test machine can be resolved into biaxial components through a geometrical correction

factor, calculated from the geometry of the moving lever arms of the frame. For the frame employed in this work the correction factor was calculated as 0.355. Stress was calculated on the assumption that all stress was uniformly distributed within the region of specimen, between the grips. This region is 28 mm square when the frame is in the initial, closed position and the sample is undeformed.

Some studies have been carried out to validate the biaxial test frame [33]. Two virtually identical tensile specimens were tested in the biaxial frame to validate that biaxial extension was occurring (each specimen was held by two of the grips using the crossed arrangement shown in Figure 14). The stress-strain curves determined are shown in Figure 14. The responses are very similar, confirming equibiaxial extension. Strain measurements made, by following the movement of a grid pattern of dots, demonstrated the biaxial nature of the strain distribution in the centre of the test-piece. FE analysis of the test specimen also supported the view that the stress and strain distributions in the centre of the specimen are equibiaxial [33]. The load correction factor was confirmed experimentally by testing uniaxial tension specimens in the test frame. The determined stress-strain curves from uniaxial tension specimens tested in the biaxial were very similar to those measured in a standard uniaxial tension test (Figure 15).

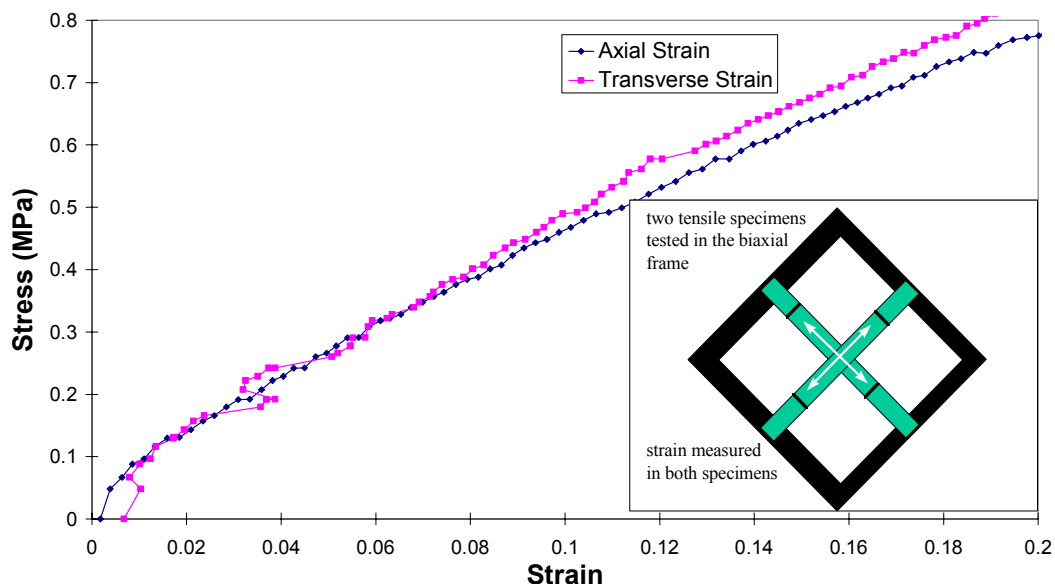


Figure 14: Validation of equibiaxial stretch from test frame

The equibiaxial test specimen is made by cutting a 45 mm square from flat sheets of bulk adhesive. The corners of the square are then removed to reduce stress concentrations between the grips. A typical test specimen, shown in the orientation in which it would be gripped, is

shown in Figure 13. The specimen shown has been tested. Gauge marks made for video extensometry are clearly visible. A crack can be seen running from the right hand edge of the specimen. The region where the specimen started to tear corresponds to the region of the specimen between the corners of the gripping blocks, where stress concentrations are highest. At large strains, thinning of the test specimen may lead to slippage in the grips.

3.3.2 Strain Measurement

Strain measurement in the biaxial test is best performed using non-contact methods such as video extensometry. Strains can be determined from the extension of two gauge marks in the vertical axis of the test machine (Figure 13) as it can be shown geometrically that in equibiaxial tension this strain is equivalent to the equibiaxial strain in specimen (which is at $\pm 45^\circ$ to the test machine axis). Strains can also be determined from the grip movement although, since the strain distribution near the grips is non-linear, these will be inherently inaccurate. Grip movement should be measured using displacement transducers attached to opposite grips. Crosshead movement cannot be easily converted into strain.

3.3.3 Biaxial Tests

When carrying out biaxial tests it is essential that the test frame and the specimen are allowed to equilibrate at the test temperature. The load cell reading should be zeroed before the specimen is clamped. It is recommended that the frame be extended empty to check for friction in the pivots and lubricated if this friction is significant.

The test speed should be set to give a local strain rate in the specimen equivalent to that in the other bulk specimen tests and in the joint being analysed. Some set-up tests may need to be performed to determine the speed setting for the specimen being tested. Strains are determined from the vertical extension of two gauge marks on the specimen using a video extensometer. Loads (F) are determined from the load cell and resolved into biaxial loads (P) using the calculated correction factor ($k = 0.35476$). Nominal stress is calculated from the measured biaxial load divided by the initial cross-section area where c is the sheet thickness and a is the initial separation of the biaxial grips (28 mm). As the cross-section area of the

specimen increases during the test the true stress will be lower than the nominal stress (N.B. ABAQUS uses the measured nominal stress data as input)

$$\text{Biaxial Stress} = \frac{P}{a c} = \frac{k f}{a c} \quad (8)$$

The measure data are formatted as nominal stress, nominal strain for input as material properties data (Section 6).

The methods outlined above describe current practice in biaxial testing. However, there are many uncertainties associated with such tests. The major uncertainty is in the interpretation of stress from the test. The calculation of biaxial stress from biaxial force divided by initial cross-section yields an averaged stress. However, the stress distribution is highly non-uniform and local stress in the centre of the specimen, where strain is biaxial, is unknown. The stress in this region can be predicted using FEA, but a number of assumptions need to be made. It has been observed that the choice of materials model can significantly influence the stress value obtained, which increases uncertainties in the test. There is no experimental method for determining local stress in the central region (unlike strain). The problems in determining stress are not confined to the biaxial frame described, but are generic to all biaxial stretching methods [41].

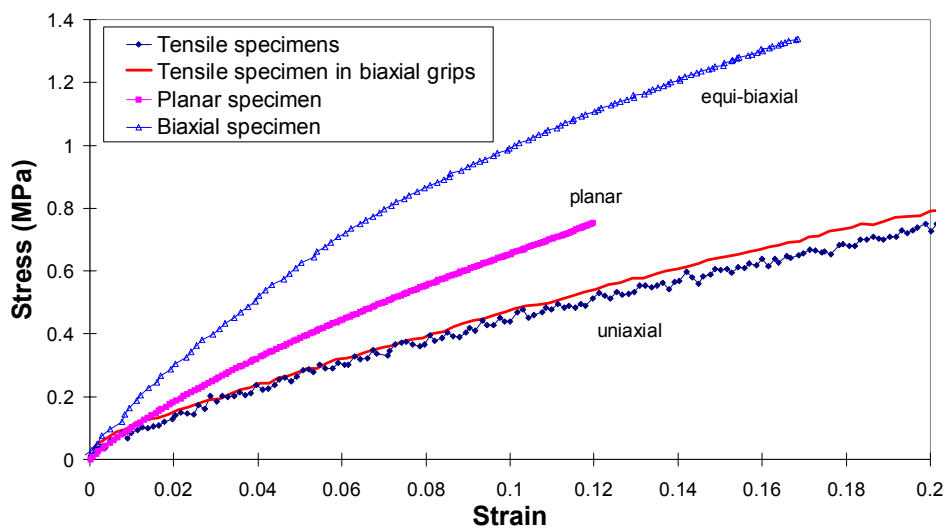


Figure 15: Comparison of stress-strain curves produced from different tension test methods

A further disadvantage with the biaxial is that the specimens fail at low average biaxial strains owing to large stress concentrations in the corners of the specimen between the ends of the grips. The strain range available from this test is limited and, again, the same problems are encountered in cruciform specimens tested on multi-axial test machines [41].

An alternative method of producing biaxial stress is through inflation of a clamped sheet of material using pneumatic pressure. This was not investigated in the current study, because interpretation of stress and strain is too complicated. There are also a number of safety implications involved in inflating specimens to failure.

3.4 Measurements for Modelling Hyperelastic Properties

Figure 15 shows a comparison between stress-strain curves produced by the uniaxial, planar and equibiaxial tension tests. As the degree of constraint and, hence, the hydrostatic stress increases the ‘stiffness’ of the test specimen increases. It is noticeable that, in comparison to the uniaxial test, the strains to failure are much reduced for the planar and equibiaxial tests.

Test data from all three of the tension test methods outlined in Section 3 are recommended for accurate modelling of multi-axial stress states using hyperelastic models [12]. Only one of the tests, the uniaxial tension, could be described as routine or readily available. The planar test specimen is large, requiring large quantities of adhesive. Specimens are also difficult to prepare. The biaxial test requires either an expensive multi-arm test machine or a special fixture. No matter which arrangement is selected there are technical difficulties in determining the biaxial stress in the specimen from measured loads. Due to the geometry and clamping of the planar and biaxial specimens, stress concentrations at the corners of the grips tend to limit the maximum strains that can be achieved in these tests. These tend to be significantly lower than strains that are measured in the uniaxial tension test. Potentially, such differences in strain ranges could destabilise numerical fitting of the data for the hyperelastic coefficients.

A series of FEA experiments was performed on a single-lap joint configuration as part of a more general investigation into factors influencing the accuracy of FEA predictions of the

force-extension behaviour of bonded joints [20]. This examined the effect of the type of input test data supplied on FE model and also factors such as material model, strain rate and temperature. The accuracy of the fit of the predicted force-extension curves to the corresponding experimental curves was evaluated through a divergence parameter. The lower the divergence parameter the better the fit. These results were analysed using a statistical design of experiments approach and the average effects of each parameter are summarised in Table 3.

Table 3: Analysis results for full experimental matrix (180 standard FEA experiments)

Level	Model	Avg Effect	Data Type	Avg Effect	Temperature	Avg Effect	Strain Rate	Avg Effect
1	Mooney-Rivlin	0.83	U	0.80	0 °C	0.84	3.00E-04	0.65
2	Ogden, N=1	0.79	UBP	0.82	20 °C	0.61	3.00E-03	0.78
3	Ogden, N=3	1.04	U+V	0.74	40 °C	0.92	3.00E-02	0.94
4	Neo Hooke	0.64	UBP+V	0.78				
5	Arruda-Boyce	0.65						

Four different combinations of input data were evaluated: uniaxial tension only (U), combined uniaxial, biaxial and planar tension (UBP), uniaxial tension and volumetric properties (U+V), as described in Section 4, and combined uniaxial, biaxial and planar tension and volumetric properties (UBP+V). Where volumetric properties data were not used the D_i volumetric coefficients in the models were by definition 0 (i.e. the materials were assumed to be incompressible). The averaged results show that there is little difference between the accuracy of predictions made using uniaxial data only and those made using the combined uniaxial, biaxial and planar tension data [20]. Therefore, it appears that the biaxial and planar tests can be omitted with little effect on accuracy, thus simplifying testing requirements. The addition of volumetric data to calculate the volumetric coefficients improves the accuracy of the fits. The best combination of input data was uniaxial tension and volumetric tension. Therefore, uniaxial tension and volumetric tension appear the most effective input data for modelling flexible adhesives. Section 4 outlines a method for obtaining volumetric properties from the uniaxial tension test, all of the required data can be obtained from a single measurement.

4. Methods for Determining Volumetric Properties

It is common when modelling natural rubbers to assume that the material is incompressible, thus the volumetric properties can be ignored. Therefore, in the hyperelastic models all the volumetric D_i coefficients can be assigned the value zero. Incompressibility corresponds to a Poisson's ratio approaching 0.5. However, measurements on flexible adhesives [1, 20] tended to indicate that Poisson's ratio values for flexible adhesives were approximately 0.30 to 0.35. Thus, the assumption of incompressibility is invalid.

When using hyperelastic material models to predict the behaviour of flexible adhesives with a Poisson's ratio of less than 0.5, it is prudent to account for the materials compressibility. This is achieved by including a volumetric term (calculated from volumetric data) along with the hyperelastic coefficients. The user manuals for ABAQUS [12] recommend that coefficients (D_i) required to define the volumetric contribution are calculated from data obtained from volumetric compression of a specimen. The volumetric compression test of a sample with known dimensions (sample radius and height) produces data in the form of a load and a piston displacement. ABAQUS requires data in a tabular form as the pressure, P , and the corresponding volume ratio, J (current volume/original volume), throughout the test.

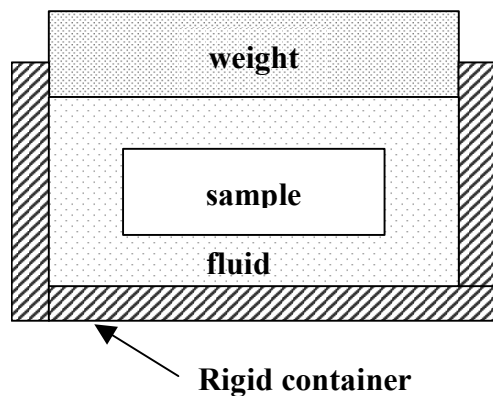


Figure 16a: *True hydrostatic compression*

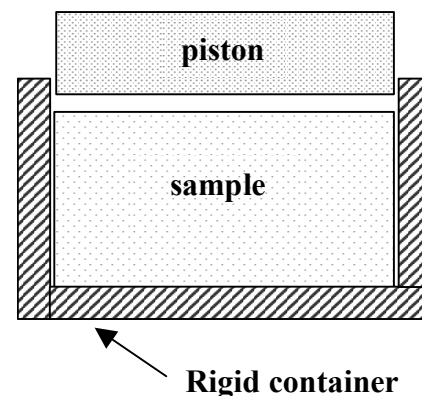


Figure 16b: *Quasi-hydrostatic compression*

4.1 Volumetric Compression

One method of measuring true volumetric compression is a dilatometer (Figure 16a). This is an application of true hydrostatic pressure. The stress is applied to a fluid and acts equally on the sample in all directions. Measurements using this method are the most accurate, but the requirement for a liquid to transmit the pressure to the sample limits the pressures range [42].

A simpler but more approximate way of conducting a volumetric compression test involves applying stress to the sample in one direction only. The sample is a small cylinder of material inside a rigid container. As the surface of the sample is compressed the sides try to move outwards in response to the stress, but are restrained by the rigid container (Figure 16b). Stresses are thus generated on the sides as well as the top and bottom of the sample. The stress field is quasi-hydrostatic as the stresses on the sides are lower than those at the top and bottom. Although both volumetric and deviatoric deformations are present, the deviatoric stresses will be several orders of magnitude smaller than the hydrostatic stresses (because the bulk modulus is much higher than the shear modulus) and can be neglected. The limitation of this type of apparatus is the stiffness and yield strength of the container [43].

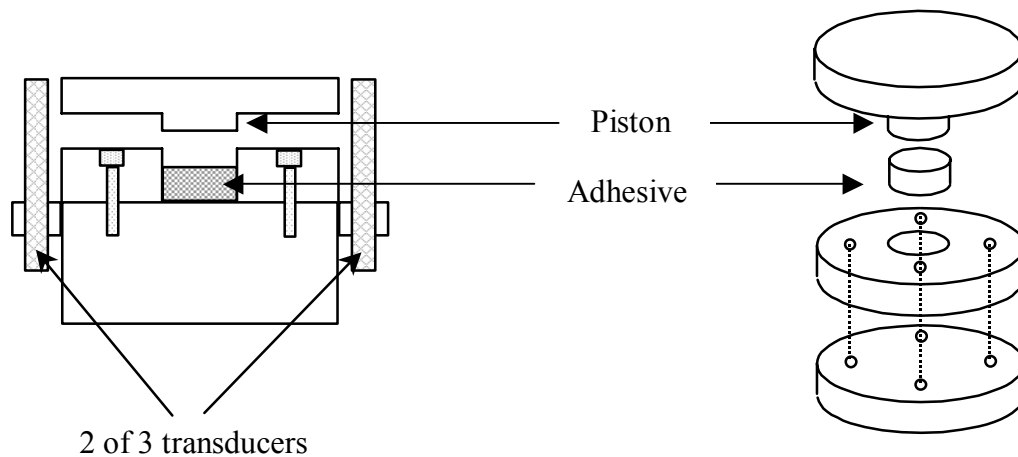


Figure 17: *Schematic of volumetric compression fixture*

Apparatus for performing a quasi-hydrostatic volumetric compression test is illustrated in Figure 17. The steel base plate, piston and cylinder are very much stiffer than the adhesive, and FEA investigations show that they deform insignificantly under test loads. The test specimen is formed within the 20 mm diameter central cylinder of the test fixture,

compressed under light pressure, using the weight of the piston to ensure a level surface, and cured in the test fixture (Figure 18). To test, the fixture is compressed between two parallel platens in a universal test machine. Three displacement transducers are clamped at three equally spaced points around the fixture. These determine the compression of the sample and provide a check for uniform compression.

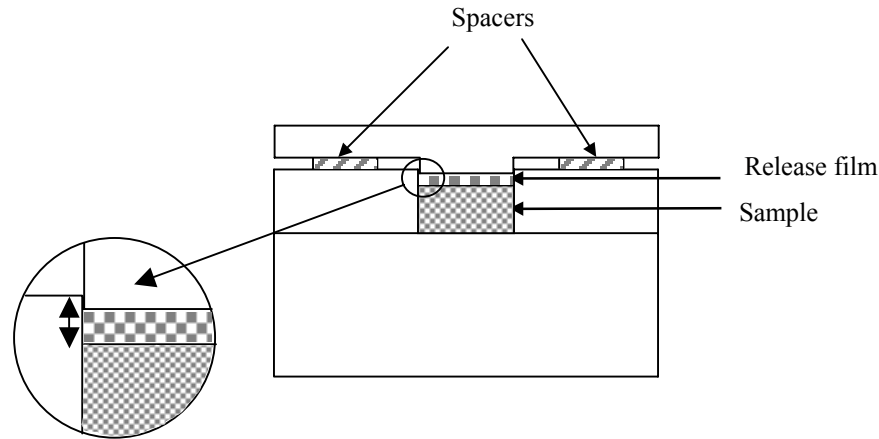


Figure 18: *Set-up for preparing volumetric compression specimen*

The compressive stress imposed by the piston is effectively the pressure data and can be calculated as

$$P = \frac{F}{\pi r^2} \quad (9)$$

where P is the pressure, F is the measured load and r is the sample radius.

The volume ratio, J , is calculated as

$$J = \frac{V}{V_0} = \frac{\pi r^2 h}{\pi r^2 h_0} = \frac{h_0 - \text{piston displacement}}{h_0} \quad (10)$$

where V = current volume, V_0 = original volume, r = sample radius, h = current sample height and h_0 = original sample height.

The calculated pressure and volume ratio data should be formatted as described in Section 6. Data are supplied as pressure, volume ratio.

4.2 Volumetric Tension

Although FEA manuals recommend the use of volumetric compression data, it is considered that properties in tension are critical to joint failure and that volumetric behaviour in tension may be more relevant. A form of volumetric data can be obtained from the uniaxial test [44]. During testing both the axial strain and transverse contraction should be obtained along with the load. From the strain measurements a form of volume ratio can be obtained, assuming that the through-thickness strain is equivalent to the transverse strain in the direction of width (i.e. $\epsilon_2 = \epsilon_3$, ϵ_2 and ϵ_3 have negative signs during tensile extension). The pressure P required by ABAQUS is equivalent in magnitude to the true tensile stress σ_T obtained from the measured load using Equation (6).

The volumetric strain can be determined from the original and current volumes of the tensile gauge volume as follows:

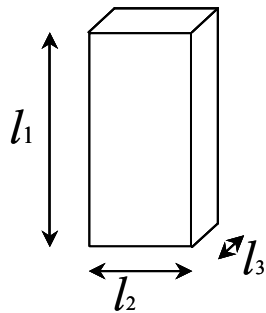


Figure 19: *Tensile volume element*

$$\text{Original volume; } V_0 = l_1 l_2 l_3 \quad (11)$$

$$\text{Current volume; } V = l_1(1 + \epsilon_1) l_2(1 + \epsilon_2) l_3(1 + \epsilon_3) \quad (12)$$

$$\text{Volume ratio } J = V/V_0 = (1 + \epsilon_1)(1 + \epsilon_2)^2 \quad (13)$$

where l_1 is the extensometer gauge length, l_2 is the specimen width, l_3 is the specimen thickness as shown in Figure 19, ϵ_1 is the axial strain and ϵ_2 is the transverse strain.

When considering tensile volumetric data, the current volume is larger than the original volume, hence $J=1$ at zero stress and increases with increasing tensile stress. As the compressive pressure is deemed positive in ABAQUS, then the tensile pressure stress should

be regarded as negative, in other words input data should be in the form $P = -\sigma$ and $J \geq 1$. When the FE analysis is carried out using these data the following ABAQUS warning message is generated “The nominal strain is opposite in sign to the stress. This is not physically reasonable”. This warning message does not imply failure of the analysis as D_i values can be successfully calculated.

An alternative approach is to calculate the inverse volume ratio giving $J \leq 1$ and using positive pressure values. In this case $J=V_0/V$ (original volume/current volume). The D_i value is calculated in this instance without a warning message. After investigation, the D values obtained from both methods were found to be comparable.

For the input data, the first data set should be pressure = 0, volume ratio = 1, although this is not compulsory. The data should be copied into a worksheet with the pressure data in the first column and the volume ratio in the second. This is then saved as a .csv format file and converted into a file called e.g. *volumetric.dat* ready for reading into the input file. An example set of volumetric tension data is provided in Appendix II.

5. Methods for Determining Visco-Elastic Properties

Flexible adhesives are visco-elastic materials, i.e. their behaviour is a combination of strain-dependent elastic (recoverable) and strain rate dependent viscous (irrecoverable) processes. The visco-elasticity provides for beneficial properties, such as damping, but can complicate the prediction of mechanical performance through strain rate and temperature sensitivity of the response and creep behaviour under constant loading conditions.

Strain rate and temperature sensitivity of the mechanical properties can be explored through tests under different conditions. Where data are available under conditions appropriate to the design then these can be used directly but in order to evaluate the joint performance under different conditions it is necessary to either measure or interpolate material properties.

It is difficult to predict the derived hyperelastic coefficients as functions of strain rate and temperature, particularly if the selected model contains several coefficients [20]. Generally, the volumetric behaviour has a minor effect on the predictions and, therefore, assuming constant values for the D_i components should not introduce excessive errors [20]. Where the model contains only one deviatoric coefficient (such as Arruda-Boyce or Neo Hooke) then there is a greater chance of deriving functions to interpolate the value of this coefficient [20]. However, if two or more fitted coefficients are required then these tend to have scattered values and cannot be accurately interpolated. In such cases it may be more effective to interpolate values from sets of stress-strain curves at different rates/temperatures to determine a 'new set of data' to use in the analyses.

Finite Element models can include rate dependency through visco-elastic functions. In ABAQUS [12], for example, rate dependent responses can be modelled as a sum of relaxations to the stiffness matrix that can be characterised from either stress relaxation or creep measurements [45-47]. The analysis must be run using a step that includes time. In ABAQUS quasi-dynamic behaviour can be modelled using a *VISCO step and full dynamic behaviour, including inertia effects, through EXPLICIT analyses.

5.1 Stress Relaxation

A stress relaxation measurement is performed by rapidly applying a strain, holding that strain constant and monitoring the load over a set period of time [45-47]. Measurements can be performed on either bulk test specimens (e.g. uniaxial tension) or joint specimens (e.g. single-lap shear). Relaxation tests can be performed using tensile test machines although for longer-term measurements a static test frame (Figure 20) where the specimen can be extended in tension by a set amount may be preferable. Although only the load data are truly needed to determine stress relaxation, it is good practice to also measure strain as this determines the strain at which the relaxation occurs (important if the relaxation function is strain dependent). This is needed to calculate relaxation modulus and can be used to confirm that the applied strain remains constant.

The data produced are time-dependent load curves, it is important that the time from the start of each test can be determined in the test record. Care should be taken when using data collection equipment that has data reduction or data collection features as the essential information on when a point was recorded may not be available. It is preferable if the time is directly recorded rather than being inferred from the data collection rate.

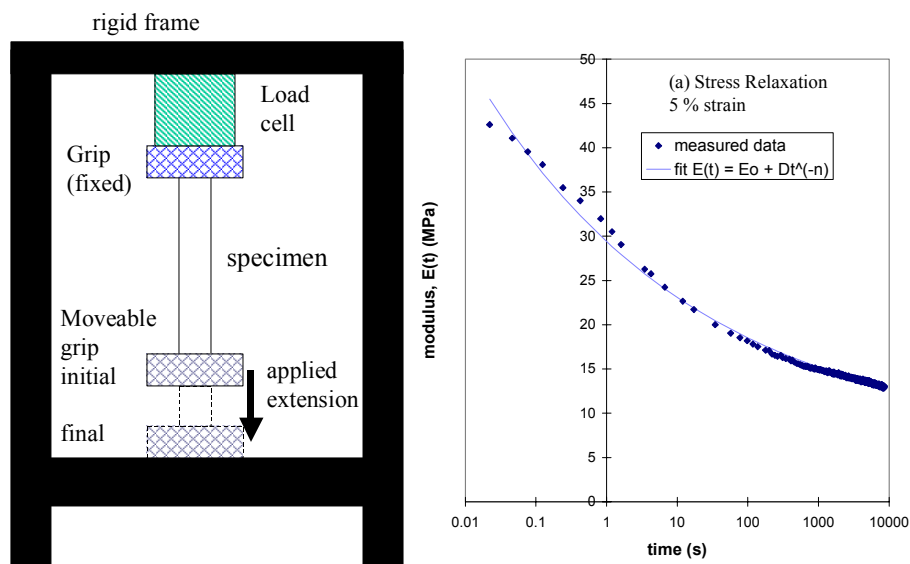


Figure 20: Schematic of relaxation test and typical results for a flexible adhesive

The point of maximum load should be designated as the start of the relaxation with the proviso that the strain after this point is constant. If the strain changes after maximum load, e.g. due to backlash in the test control system, then the point where strain becomes constant should be taken as the start of the relaxation. Subsequent test times should be adjusted for this point of zero relaxation. It is usual to calculate the relaxation modulus from the measured load, applied constant strain value and specimen dimensions. The results should be normalised by the relaxation modulus at the defined start of the relaxation. Thus the normalised relaxation modulus decreases from one with increasing time. The initial point (at zero time) should be omitted from the data used to fit the FE relaxation function to avoid fitting errors. It is also normal practice to omit points occurring within a period of time equal to three times the period of load application, as these may be unreliable. Thus, short-time relaxation phenomena need to be characterised with tests where the load is applied rapidly.

5.2 Creep

Creep [45] is the time-dependent deformation resulting from the application of a constant stress on a component (although constant stress is often taken as constant load). This can be measured on bulk or joint test specimens although with flexible adhesives both types of specimen present measurement problems [46-48]. The key to creep measurement is accurate and stable measurement of strain. It is also important to maintain a stable temperature. Tests are normally terminated when one of three conditions are met; either (i) the test exceeds a pre-determined duration, (ii) the strain exceeds a pre-determined value or (iii) the specimen ruptures.

5.2.1 Creep Test Apparatus

Uniaxial tensile test specimens have very low stiffness and, hence, present problems for loading. The applied force needs to be low so as not to exceed the static failure strength of the material. Deadweight loading of the specimen (Figure 21a) is the most straightforward method of performing a creep test. However, unless some sort of frictionless guide is used, hanging a load from the specimen will tend to cause the specimen and grips to swing when the load is applied leading to very poor measurement accuracy [45]. A preferred arrangement is to apply the load via a lever arm at the top of the specimen (Figure 21b). This tends to

reduce movement of the specimen. Force should be applied slowly to avoid the system oscillating.

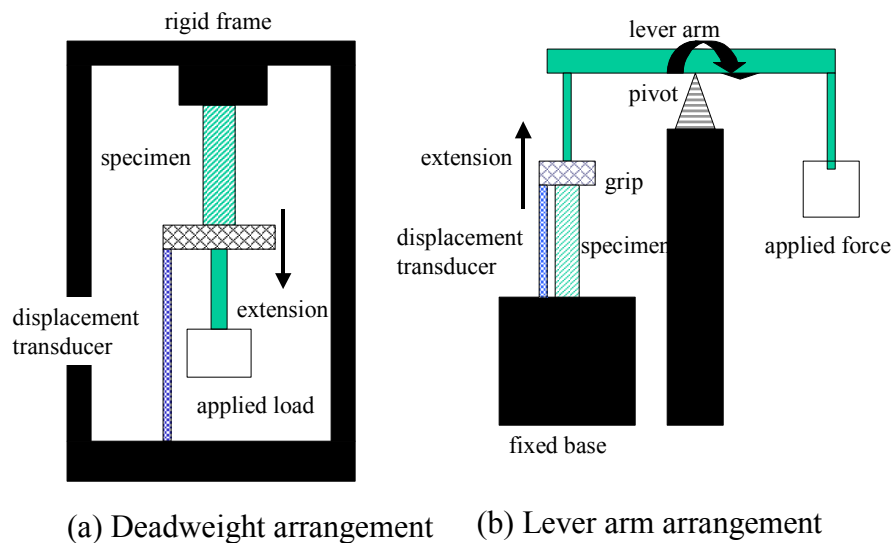


Figure 21: *Schematics of creep tests*

5.2.2 Strain Determination

Extensometry presents a problem – video extensometers could be used, but this is uneconomic. Normal practice is to use a long-travel displacement transducer to measure the movement of the moving grip. This gives extension, but not local strain. Correction functions to obtain strains from grip movement can be applied using methods outlined in Section 3.1. However, as the relaxation function requires strain values that are normalised by the elastic (or initial) strain and provided the strain-extension function is approximately linear then extensions can be used instead of strains.

In joint specimens small displacements make accurate strain determination difficult. It is advisable to attach accurate extensometers that straddle the bond line of the specimen rather than measure grip movement in order to exclude any extraneous movements that have a major influence on the results.

The measured creep data need to be converted into a creep-time, normalised strain format [45] to determine the relaxation function that models the time-dependence of the matrix stiffness. The initial ‘elastic’ strain (or extension) defined by the elastic properties needs to

be identified on the strain (or extension) vs. time plot. This is defined as zero creep time and all subsequent test times are adjusted accordingly. All strains (or extensions) are normalised by dividing by this value. The initial strain is identified as a point of inflection on the curve where high rate elastic response gives way to lower rate creep responses. As Figure 22 illustrates, it is not easy to precisely define the point that is the initial ‘elastic’ strain. Uncertainties in this value can cause large uncertainties in normalised creep strain values. The zero time point should be excluded from the input data, as this will cause a fit error. Thus, the data set consists of a set of normalised strains whose initial value is greater than one and increases with time. An example creep data set is shown in Appendix II.

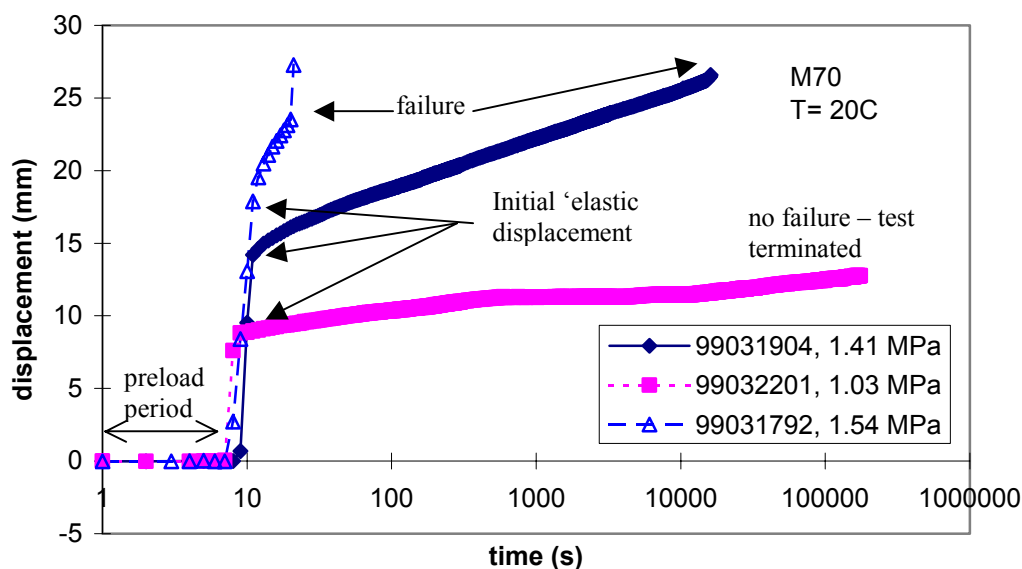


Figure 22: Typical flexible adhesive creep measurements

5.2.3 Creep Rupture

Creep rupture tests, also known as static fatigue tests, are often performed to evaluate durability of joints under static loading. By loading at different proportions of the static strength of the joint and determining time to failure (which will decrease as the load increases) durability can be assessed. Thus, creep tests can provide information on the failure of joints, unlike relaxation tests. Results of creep tests performed on bulk uniaxial tension specimens of a flexible adhesive at different temperatures and loads [46] are shown in Figure 23. These are plotted as failure strain against applied stress. Quasi-static failure values are added for comparison. It can be seen that the creep and the static results follow a similar

envelope. It is possible that low rate static tests at elevated temperatures can provide a means of evaluating maximum static stresses for joints.

5.3 Rate and Time Dependent Predictions

Input data, for predicting the rate and time dependent response of a joint bonded using a flexible adhesive, are obtained more accurately from stress relaxation tests than they are from creep tests. A fundamental problem with tensile creep test is that, as the extension increases, Poisson's contraction of the specimen will reduce the loaded area and the true stress will increase. Thus, the test is at constant load, but not constant stress and the creep strain rate will accelerate as the test proceeds. Load measurements can be made more reliably in stress relaxation than strain measurements in creep. The identification of the initial elastic response tends to be easier as the maximum load in stress relaxation is normally more readily identifiable than the inflection at the elastic strain in creep tests. The easier identification of the initial point provides higher confidence in the responses determined at short times. However, creep tests would be required to evaluate long-term durability.

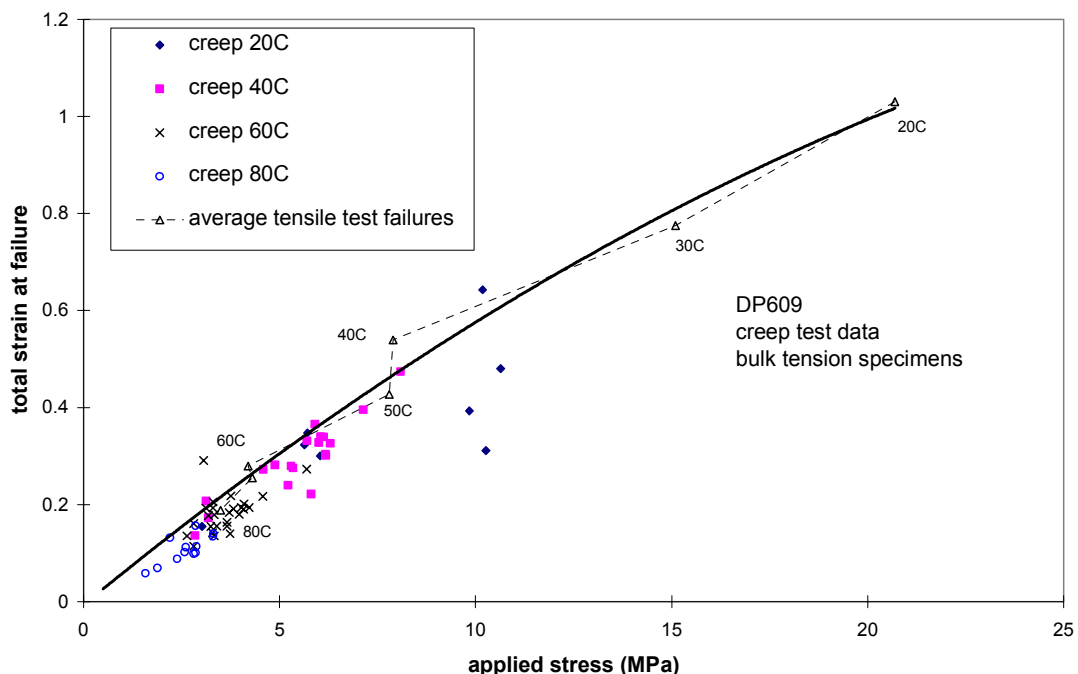


Figure 23: Failure data determined from creep and quasi-static tests

Rate dependence in monotonic loading can be handled in the FE analyses through visco-elastic or time-dependent properties. In the ABAQUS FE package [12] the time-dependence

of modulus can be included in the material properties definition through the ABAQUS *VISCOELASTIC command and examples of visco-elastic material property definitions are shown in Appendix II.

An example of this approach is shown in Figure 24. FE predictions made for a comparatively slow strain rate using a standard static analysis (*STATIC) and material properties obtained at the low strain rate are compared with a quasi-dynamic analysis (*VISCO) using higher strain rate properties combined with visco-elastic relaxation. Time-dependent properties of the adhesive had been obtained from a stress-relaxation test on a bulk tensile specimen extended to 5 % strain [1]. The time-dependent loads were normalised by the initial load in order to format the results for input into the FE model. The visco-elastic prediction was very similar to the time-independent *STATIC prediction of the lap joint response at the comparable strain rate ($3 \times 10^{-4} \text{ s}^{-1}$). The quasi-dynamic analysis of the model run using low strain rate input properties and no visco-elastic relaxation gives exactly the same predictions as the static analysis.

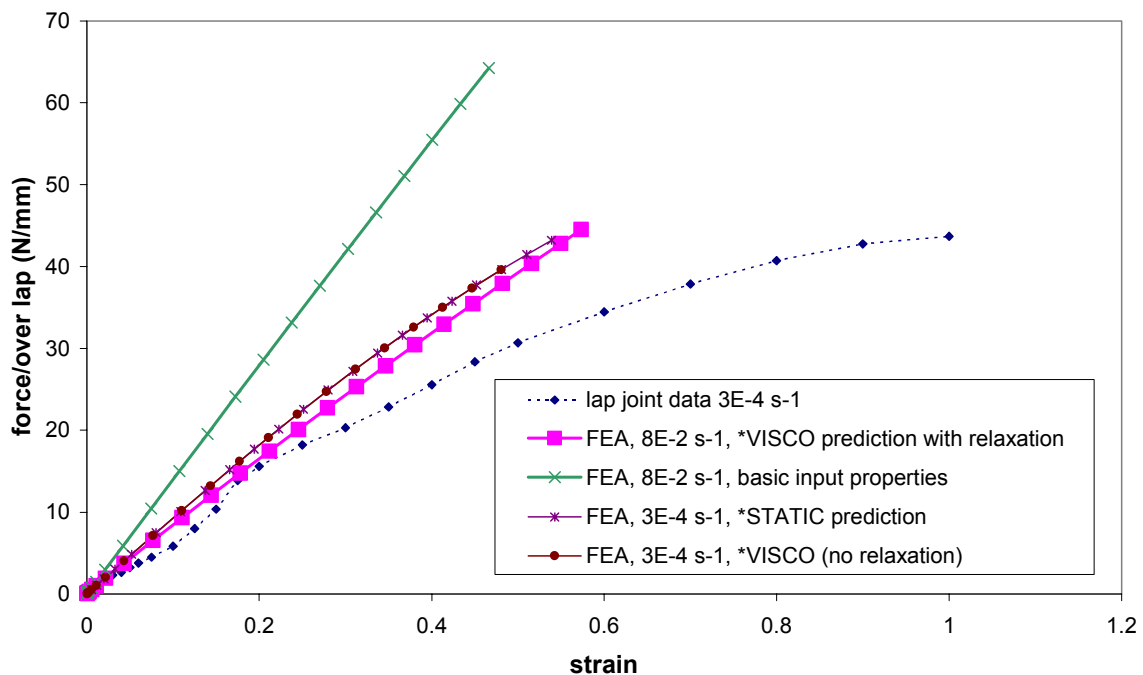


Figure 24: Comparing static and quasi-dynamic FEA predictions

6. Formatting Data For Hyperelastic Materials

6.1 Presenting Experimental Data

6.1.1 Uniaxial, Biaxial and Planar data

A convenient method for defining a hyperelastic material is to supply the FE program with experimental data. The constants are then calculated using a least-squares method. Various combinations of uniaxial tension, biaxial tension and planar tension data can be used to derive the coefficients. This section explains the data manipulation necessary in order to obtain data in the format required by the FE program ABAQUS [12].

The uniaxial, biaxial and planar tension tests all produce raw data in the format of load and extension, with known specimen width, thickness and gauge length for each sample tested. ABAQUS requires the data in the tabular form of a series of nominal stress and nominal strain data sets. These data can be calculated as shown below.

For all three test methods the strain is calculated as

$$\varepsilon = \frac{\delta L}{L} \quad (14)$$

where ε = nominal strain, δL is the measured extension (mm) and L is the original gauge length (mm).

Nominal stresses are calculated from uniaxial and planar data as

$$\sigma = \frac{F}{w t} \quad (15)$$

where σ is nominal stress, F is force measured in load cell, w is sample width and t is sample thickness.

With the biaxial data, the biaxial nominal stress is calculated as follows

$$\sigma_b = \frac{k F}{a c} \quad (16)$$

where F is the force measured by the load cell, k is the geometrical correction factor derived from the lever ratios in the scissored frame (0.35476 for the frame used), σ_b is the nominal biaxial stress, a is the initial grip separation (28 mm) and c is the sample thickness.

The above equations should be used to convert all the load, extension data into nominal stress and nominal strain data.

Some data values may have been recorded prior to the start of the test so the next step is to pinpoint the start of the test and remove the preceding data. The FE program requires that the all data set values are positive. The raw stress and strain data can be adjusted by translation so that the data at the start of the test are nominal stress = 0 and nominal strain = 0. Next, identify the failure point of the test specimen and remove the subsequent stress and strain data.

These adjusted stress and strain data should be copied to a blank spreadsheet, placing the nominal stress values in the first column and the nominal strain values in the second column with no column headings. This spreadsheet should be saved as a comma delimited (.csv) file, which puts a comma between the two values in each data set.

In order to calculate model coefficients in the ABAQUS FEA package as outlined in Appendix III, comma separated variables format (.csv) files containing stress-strain data for each uniaxial, biaxial and planar failure should be converted to Unix format and re-named *uniaxial.dat*, *biaxial.dat* and *planar.dat* respectively, ready for reading into the input file. This conversion is carried out in Unix using the command *to_unix filename.csv filename.dat*. The use of these files is explained in Section 6.2 and an example set of uniaxial data is shown in Appendix II.

6.1.2 Volumetric Data

The calculated pressure and volume ratio data should be formatted as described in Section 6.1.1. Any data recorded prior to the start of the test should be removed, along with data recorded after specimen failure (taken as the point of maximum load). When considering tensile volumetric data, the current volume is larger than the original volume, hence $J = 1$ at zero stress and increases with increasing tensile stress. As the compressive pressure is deemed positive in ABAQUS, then the tensile pressure stress should be regarded as negative, in other words supplying input data in the form $P = -\sigma$ and $J \geq 1$. When the FE analysis is carried out using these data the following ABAQUS warning message is generated “The nominal strain is opposite in sign to the stress. This is not physically reasonable”. The presence of this warning message does not cause failure of the analysis, and D values are successfully calculated.

An alternative approach is to calculate the inverse volume ratio giving $J \leq 1$ and using positive pressure values. In this case $J = V_0/V$ (original volume/current volume). D values are calculated in this instance without a warning message. After investigation, the D values obtained from both methods were found to be comparable.

For the input data, the first data set should be pressure = 0, volume ratio = 1, although this is not compulsory. The data should be copied into a worksheet with the pressure data in the first column and the volume ratio in the second. This is then saved as a .csv file and converted into a file called e.g. *volumetric.dat* ready for reading into the input file. An example set of volumetric tension data is provided in Appendix II.

6.1.3 Visco-Elastic Data

Visco-elastic data can be supplied as either stress relaxation or creep data. In each case the results should be normalised with respect to the initial ‘elastic’ value. All data before and including this initial elastic point should be removed from the data set. The time of the initial ‘elastic’ point should be subtracted from the subsequent experimental times and the data file should be formatted as pairs of normalised visco-elastic value N , normalised time t . For stress relaxation data $N < 1$ and decreases with time. For creep data $N > 1$ and increases with

time. This data file should be saved as a .csv file and then converted into a Unix file, e.g. *visc.dat*. Visco-elastic properties can be added to either elastic or hyperelastic material properties. The material properties definitions in the input file follow the format:

*HYPERELASTIC (or *ELASTIC)

hyperelastic (or elastic) material properties

*VISCO-ELASTIC

visco-elastic properties

Examples of material properties definitions are shown in Appendix II.

6.2 Calculating Hyperelastic Coefficients

An FE analysis is run to obtain the hyperelastic coefficients. The analysis extracts the experimental data from the relevant .dat files and performs a least-squares fit procedure to obtain the coefficients. This procedure minimises the relative error in stress. An example of an ABAQUS input file is shown in Appendix III. This input file contains ABAQUS commands for calculating coefficients for all the available ABAQUS hyperelastic models [12]: polynomial, Mooney-Rivlin, reduced polynomial, Neo Hookean, Yeoh, Ogden, Van der Waals and Arruda-Boyce. Various combinations of uniaxial, biaxial and planar data can be used: uniaxial only; uniaxial and biaxial; uniaxial and planar; uniaxial, biaxial and planar; biaxial only; biaxial and planar (planar data cannot be analysed alone). Each of these combinations can be run either with or without volumetric data although including volumetric data makes no difference to the calculated deviatoric coefficients.

Only one set of coefficients can be calculated per analysis run, therefore the input file must be modified to select the required analysis type prior to running the analysis. The unused analysis types can be de-selected by typing ** at the start of each line. The input file example shows the Mooney-Rivlin analysis selected and all others de-selected. The command *INCLUDE,INPUT=filename.dat is used to extract the experimental data from the .dat files. The .dat files must be saved in the same Unix directory as the input file. An alternative is to include the tabular data directly under the model definition command. Once the analysis has

finished running, open the file jobname.dat (e.g. coefcalc.dat). It is worth checking for any stability warnings and note these. An example is shown below:

*****WARNING: UNSTABLE HYPERELASTIC MATERIAL**

FOR UNIAXIAL TENSION WITH A NOMINAL STRAIN LARGER THAN 0.4500
 FOR UNIAXIAL COMPRESSION WITH A NOMINAL STRAIN LESS THAN -0.3056
 FOR BIAXIAL TENSION WITH A NOMINAL STRAIN LARGER THAN 0.2000
 FOR BIAXIAL COMPRESSION WITH A NOMINAL STRAIN LESS THAN -0.1695
 FOR PLANE TENSION WITH A NOMINAL STRAIN LARGER THAN 0.3700
 FOR PLANE COMPRESSION WITH A NOMINAL STRAIN LESS THAN -0.2701

Then a search for the word ‘hyperelasticity’ finds the section listing the calculated coefficients, an example of which is shown below:

HYPERELASTICITY - MOONEY-RIVLIN STRAIN ENERGY

D1 C10 C01
 7.442617E-03 4.713647E-02 2.13972

Table 4 Hyperelastic coefficients from a selection of models.

‘-’ indicates a coefficient that is not relevant to a particular model

	D ₁	C ₁₀	C ₀₁	μ ₁	α ₁	λ ₁
Mooney-Rivlin	0.0383	0.0471	2.140	-	-	-
Ogden N=1	0.0383	-	-	4.413	-2.008	-
Neo Hooke	0.0383	2.01968	-	-	-	-
Arruda-Boyce	0.0343	-	-	3.987	-	7.005

Table 4 shows example coefficients for a selection of models. These were obtained for an elastomeric adhesive at a testing temperature of 20 °C and test rate of 10 mm/min, using uniaxial, biaxial, planar and volumetric data.

6.3 Single Element Check

A single 3-dimensional continuum reduced-integration, hybrid C3D8RH element with unit dimension can be used to evaluate the hyperelastic model coefficients. The single element can be subjected to uniaxial tension, biaxial tension and planar tension to obtain predictions to compare directly with the experimental data used to calculate the coefficients. An example of the single-element input file is shown in Appendix IV. The three loading situations are described in different steps. Step 1 applies uniaxial tension, step 3 applies biaxial tension, step 5 applies planar tension. Steps 2 and 4 return the element to its original state ready for re-loading.

There are two options for defining the material model. The calculated coefficients can be entered using the command `*HYPERELASTIC, modelname` with the coefficients defined on the following line or the experimental data can be referenced as before using the `*HYPERELASTIC, modelname`, `TEST DATA INPUT`, and `*INPUT, INCLUDE = filename.dat` commands so that the coefficients are calculated during the analysis. The example file in Appendix IV shows the coefficients (from uniaxial and volumetric data only) for a Mooney-Rivlin analysis entered directly. Once the analysis has run the stress and strain predictions for each step and, hence, each loading condition can be obtained directly from the reaction force, RF1 at node 2, and displacement, U1 at node 2 (as area = 1*1 and gauge length=1). These predictions should then be plotted against the experimental data.

A reasonable correlation between experimental and predicted data increases confidence in the coefficients. An example of the comparison that is attainable between predicted and experimental data is shown in Figure 25. The data shown are for an elastomeric adhesive tested at 20 °C and a test strain rate of $3 \times 10^{-3} \text{ s}^{-1}$ (equivalent to 10 mm/min uniaxial tension test speed). Good correlation is obtained for both the uniaxial and planar tests, with only moderate correlation for the biaxial test.

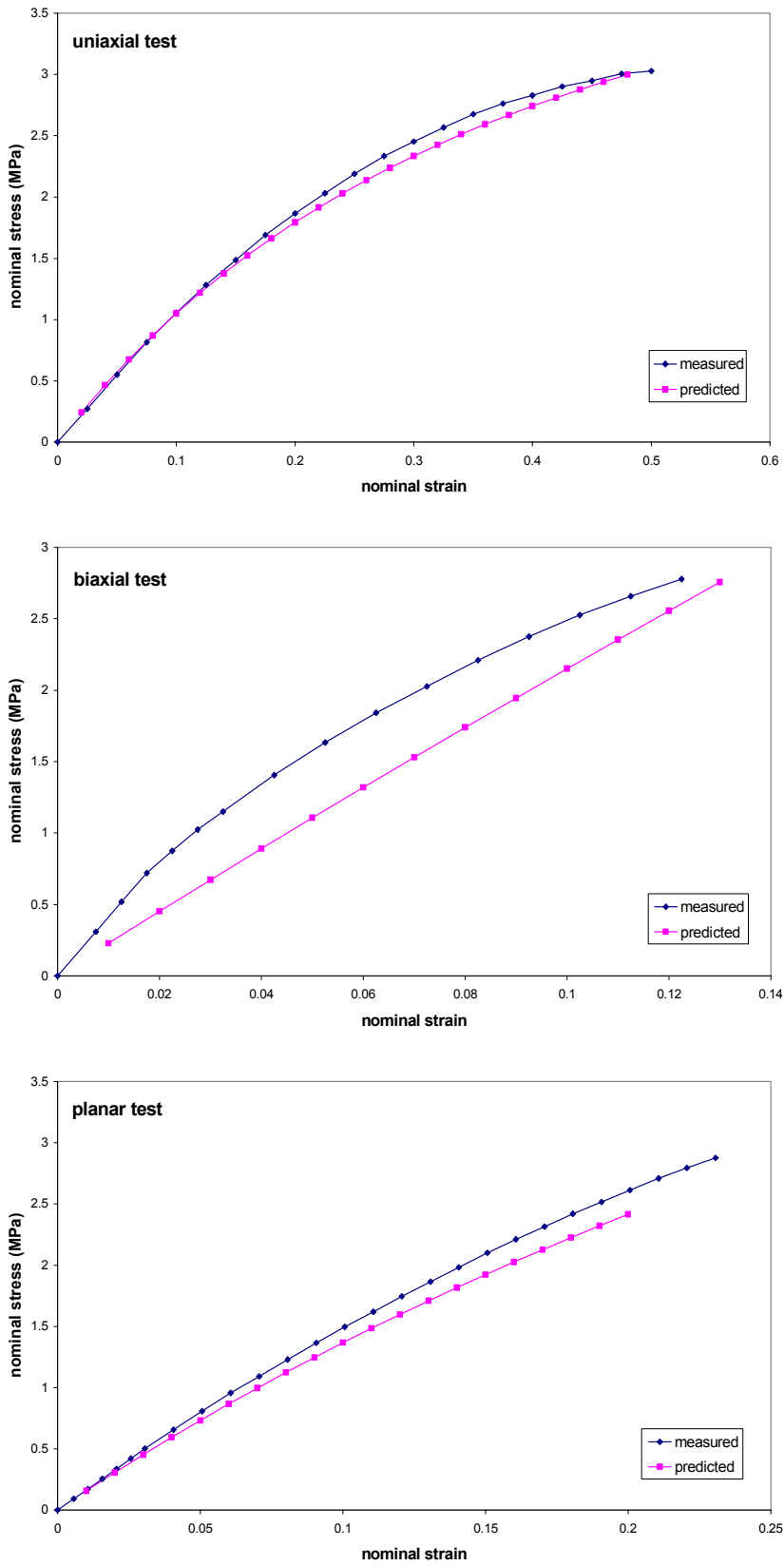


Figure 25 *Nominal stress-nominal strain plots showing the comparisons between hyperelastic test data and Mooney-Rivlin predictions for uniaxial, biaxial and planar tests*

7. Finite Element Modelling

7.1 Comparison of Element Types

In any Finite Element model there tends to be a compromise between accurate representation of the component and available computational resources. If symmetry allows, many adhesive joint configurations are commonly represented by 2-dimensional models (with width ignored) rather than 3-dimensional models in order to reduce run times and limit analysis file sizes. Two-dimension FE elements can be broken down into three generic types – plane stress (PS), plane strain (PE) and generalised plane strain (GPE). Plane stress elements are recommended for thin or unconstrained components and are not considered suitable for adhesive layers. Plane strain elements are recommended for thick or constrained components (e.g. an adhesive layer). Generalised plane strain elements are similar to plane strain elements, but allow for some Poisson's contraction.

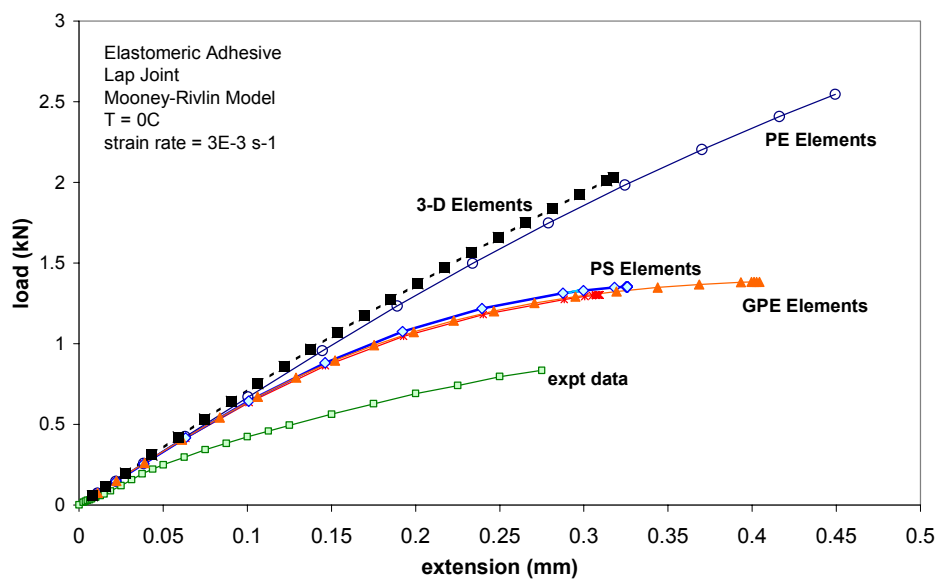


Figure 26: Comparison of different element types

Predictions of the load-displacement response of a single-lap joint made using the three types of 2-dimensional elements are shown in Figure 26. The PE element predictions are closest to the 3-dimensional predictions. However, the PS and GPE predictions are very similar and are closer to the experimental data. The 3-dimensional contour plots showed no through-width distribution of either stress or strain and indicated that a 2-dimensional representation should be adequate. There were few differences between maximum stress values, at joint failure

loads, predicted by either PE or GPE elements [48]. Further information on element types is in Appendix V.

7.2 Material Models

Various types of hyperelastic material models are described in Appendix I. It is believed that, since flexible adhesives are relatively low strain materials in comparison to natural or synthetic rubbers, first order material models may be most suitable. It is not possible to recommend any universal material model since the behaviour of flexible adhesives is likely to be variable. It is recommended, however, that single element tests (Appendix IV) be performed to screen candidate models. The choice of material model should be validated using coupon tests to increase confidence in the design.

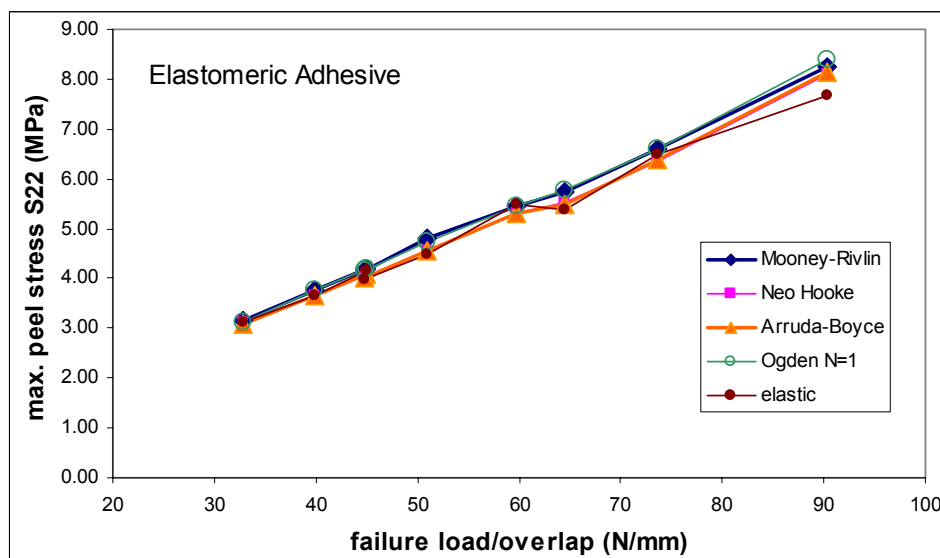


Figure 27: *Effect of material model on predicted stress concentration*

It has been observed that the choice of material model influences the shapes of the predicted force-extension curves [20]. However, at constant forces, the stress distribution does not seem to be significantly dependent on the material model as shown in Figure 27.

In models where no numerical singularities occur (often related to rounded edges and interfaces) then the maximum stress contour will cover several elements. Such stress predictions will have much less dependence on element size.

8. Failure Criteria

Appropriate materials models, accurate material properties data and valid failure criteria are required to accurately predict the strength of a bonded joint. Since the properties of the adhesive are sensitive to strain rate and temperature, it follows that the strength of joints will also depend on strain rate and temperature. Joint strength appears to decrease with increasing temperature and decreasing strain rate. This, qualitatively, agrees with uniaxial tension strength measurements. If the bond fails through cohesive rupture of the adhesive layer then there could be a direct correlation between joint strength and tensile strength.

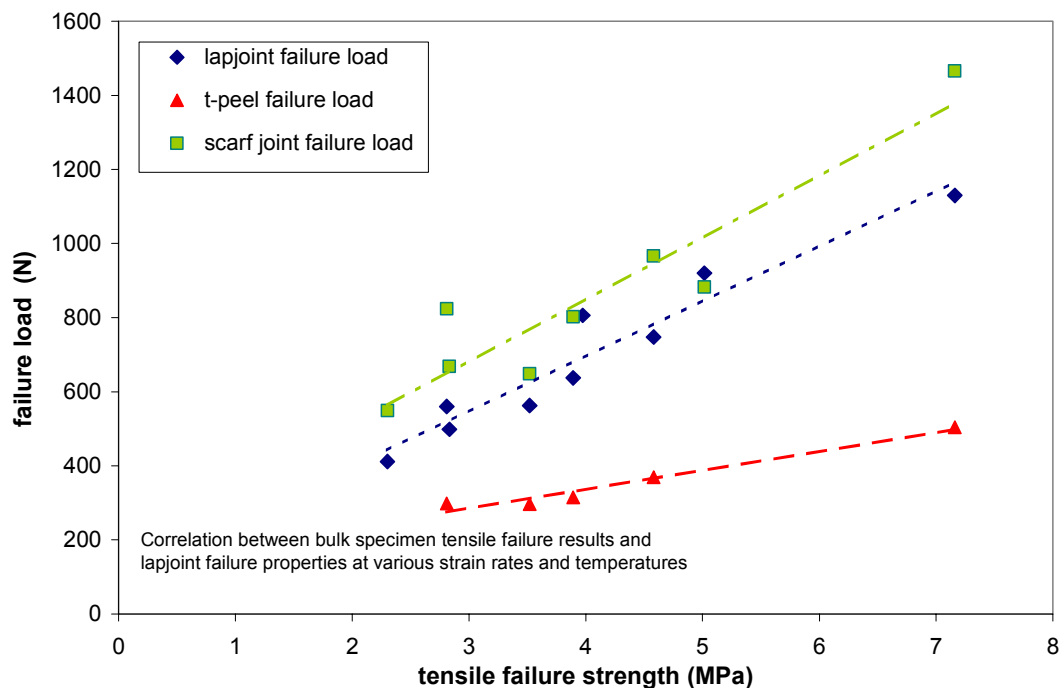


Figure 29: *Correlation between failure loads and tensile strength for elastomer adhesive*

Figure 29 shows such a correlation between maximum loads determined in tests on three different types of joint bonded with an elastomeric adhesive, performed at different strain rates and temperatures, and the corresponding tensile strengths [49]. There is a linear

relationship between joint strength and tensile strength. The failure strength of adhesive joints depends on various bond geometrical parameters, in particular bonded area [50].

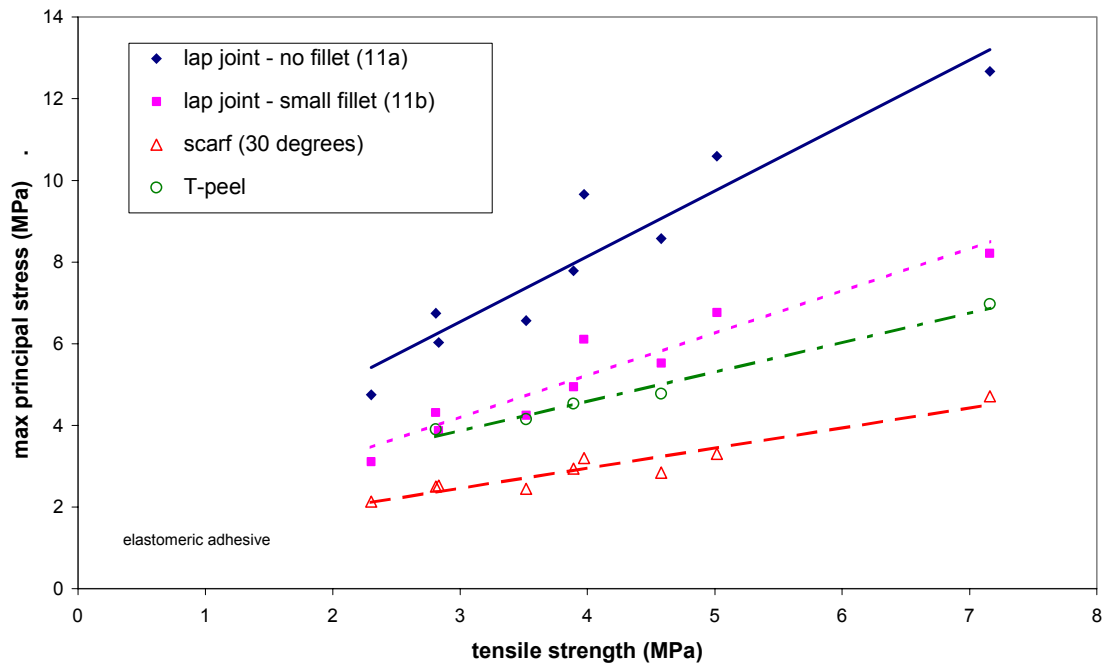


Figure 30: *Correlation of predicted maximum principal stress and tensile strength values at different strain rates and temperatures for elastomeric adhesive joints*

The existence of such a direct correlation between bulk material strength and joint strength perhaps suggests that there could be a general failure criterion for the adhesive. FEA was performed on the joints using materials data measured at the appropriate strain rates and temperatures. The predicted stress and strain distributions in the adhesive layer were analysed to determine the maximum values of components, such as maximum principal stress, maximum principal strain, von Mises stress and strain energies, at the average failure load of the joint specimen. These values were compared for different joint configurations and related to the bulk material properties [49]. There did not seem to be a single component of either stress, strain or strain energy that had a consistent value in different specimen geometries. For example, maximum principal values predicted at various strain rates and temperatures are plotted against tensile strength in Figure 30. There is a reasonable linear correlation between predicted stress values and measured tensile strengths for each joint type. However, there is no real correlation between the different types of joint geometry investigated, single lap joint [51-53], scarf joint [54] and T-peel joint [55, 56]. This lack of correlation may be due, to some extent, to the dependency of stress concentration predictions

on the size of FE element used. Stress values tended to be highly concentrated in a single element in the bond layer by sharp corners in the adherends in the lap joints and scarf joints. Only in the T-peel joints did the predicted region of maximum stress cover several elements. It is noticeable that the addition of a fillet to the FEA model produces a significant reduction in the predicted stress at the same failure load even though, a reduced element size was needed to model the fillet. Experimentally, the strength of lap joints increases if there is a fillet at the end of the bond line, but the increase is not as great as the differences between the stress values suggest. Similar findings have been observed for other adhesives.

It was found that, when different adhesives were compared in the same joint configurations, that the maximum principal stress at failure as a proportion of tensile strength varied between adhesives. In adhesive systems where the failure was not always cohesive the maximum predicted stress tended to be lower as a proportion of the tensile strength than in systems where failure was always cohesive.

The initiation and growth of cracks in the adhesive layer prior to failure has been observed in flexible adhesive joints. Design practice should consider the conditions where these cracks form, rather than conditions when the ultimate load is reached, as the operating limit of the bonded structure.

Given the uncertainty in the interpretation of the FEA stress concentrations and the potential inaccuracy of the material models used to characterise the flexible adhesives, it is unrealistic to define a definitive failure criterion. Indeed, in the light of material variability and potential degradation on ageing, this could be positively misleading. The maximum principal stress is probably as suitable as any of the criteria investigated. This seems to scale with material strength in different joint types. The maximum allowable ‘maximum principal stress’ in the joint should not exceed a defined fraction of the tensile strength of the material. Some adhesives appear to tolerate stress levels at a higher proportion of their tensile strength than others. Therefore, the scaling factor for strength would have to be decided on an adhesive-by-adhesive basis (adherend type, surface pre-treatment, etc. would also need to be considered).

9. Concluding Remarks

Test methods, that can be used to determine material properties for design with flexible adhesives, have been outlined. Three tension test methods (uniaxial, planar and equibiaxial) and two volumetric methods (compression and tension) have been described. Comparisons between predicted and experimental joint behaviours suggest that data need only be obtained from uniaxial tension test. Both uniaxial tension and volumetric tension data can be obtained from this test, which is relatively straightforward to perform. There is no appreciable gain in accuracy obtained by including the extra test data. Flexible adhesives are compressible and volumetric terms need to be included in the material models. Data for these can be determined from contraction measurements in uniaxial tension tests.

The properties of flexible adhesives depend on temperature and strain rate. Therefore, design models should be supplied with input data corresponding to the rates and temperatures under which they are to be modelled. Test methods for time-dependent properties have been described. The failure strength is strain rate and temperature dependent. There are correlations between the loads under which joints fail and the tensile strength of the adhesives under corresponding conditions. A conservative estimation of strength can be made through testing the adhesive or joint at an elevated temperature and slow test speed. It should be possible to use a time-temperature superposition approach to predict strengths. The elevated temperature/slow strain rate testing approach could also be used for the estimation of creep strengths.

Flexible adhesives can be modelled using hyperelastic material models, although the predictions of the behaviour of the bonded joints can be inaccurate and it is therefore recommended that validation tests on single elements and coupon specimens be performed to assess suitability. In general, first-order material models such as Arruda-Boyce, Mooney-Rivlin or Neo Hooke seem most appropriate for flexible adhesives. The predicted stress distributions and concentrations in the adhesive bond layer do not appear to have any significant dependence on material model, general element type or input data types, which are factors that affect the predicted force-extension behaviour. The predicted stress distributions and concentrations in the adhesive bond layer depend on joint end geometries and element sizes, which are factors that have only a limited influence on the predicted force-extension

behaviour. 2-dimensional plane strain element predictions tend to be in good agreement with 3-dimensional model predictions. However, generalised plane strain element predictions tend to show higher curvatures and, thus, better match the experimental measurements.

The strength of flexible adhesive joints depends on joint geometry. The addition of a fillet reduces the stress concentration at the end of the lap joint specimen and improves load-bearing capacity. The shape and size of the fillet influences joint strength although once fillets are over a certain size (length and height approximately twice the bond line thickness) the fillet geometry becomes less important [20].

Failure of the adhesive joints occurs under a complex, multi-axial state of stress. A simple criterion that correlates failure between different joint types or geometries has yet to be identified. Maximum principal stress correlates well with tensile strength when a single type of joint and adhesive system is investigated. Having the predicted maximum principal stress lower than the tensile strength scaled by an adhesive dependent factor of less than one may be a reasonable design criterion. However, initial crack formation in the adhesive layer has been observed to occur significantly below the ultimate strength of the joints. This should be considered when selecting design criteria to avoid this happening in service.

10. Useful Contacts

NPL

National Physical Laboratory
Queen's Road, Teddington
Middlesex, UK, TW11 0LW
Tel: 020 8943 6701

AEA Technology

Harwell
Didcot
Oxfordshire, UK, OX11 0RA
Tel: 01235 821111

ASTM

American Society for Testing and Materials
100 Barr Harbor Drive
West Conshohocken
Pennsylvania 19428
USA
Tel: 001 610 832 9500

TWI

(formerly The Welding Institute)
Granta Park
Great Abington,
Cambridge, UK, CB1 6AL
Tel: 01223 891162

IoM

Institute of Materials
1 Carlton House Terrace
London, UK, SW1Y 5DB
Tel: 020 7976 1338

SATRA

SATRA Footwear Technology Centre
SATRA House
Rockingham Road
Kettering, Northants, UK, NN16 9JH
Tel: 01536 410000

Society for Adhesion and Adhesives

(Contact: Institute of Materials)

ISO

International Standards Organisation
1 Rue de Varembe
Case Postale 56
CH-1211 Genève
Switzerland
Tel: +41 22 74901 11

MERL

Materials Engineering Research Laboratory Ltd
Tamworth Road
Hertford
Hertfordshire, UK, SG13 7DG
Tel: 01992 500 120

BSI

British Standards Institution
British Standards House
389 Chiswick High Road
London, UK, W4 4AL
Tel: 020 8996 9000

QinetiQ

(Formerly Defence Evaluation and Research Agency)
Structural Materials Centre
Farnborough
Hampshire, UK, GU14 0LX
Tel: 01252 393 300

ISE

Institute of Structural Engineers
11 Upper Belgrave Street
London, UK, SW1X 8BH
Tel: 020 7235 4535

PIRA

Pira International
Randalls Road
Leatherhead, Surrey, UK, KT22 7RU
Tel: 01372 802000

11. References

1. Duncan B, Hinopoulos H, Ogilvy-Robb K and Arranz E, Rate and temperature dependent properties of a flexible adhesive, CMMT(A)262, 2000.
2. Dean G and Duncan B, Preparation and testing of bulk specimens of adhesives, NPL Good Practice Guide No 17, 1998.
3. Broughton W, Durability performance of adhesive joints, NPL Good Practice Guide No 28, 1999.
4. Broughton W and Gower M, Preparation and testing of adhesive joints, NPL Good Practice Guide No 47, 2001.
5. Dean G and Crocker L, The use of Finite Element methods for design with adhesives, NPL Good Practice Guide in preparation, 2001.
6. Treloar L R G, Trans. Faraday Soc., vol 40, 1944.
7. Arruda E M and Boyce M C, "A three-dimensional constitutive model for the large stretch behavior of rubber elastic materials", J. Mech. Phys. Solids, vol. 41(2), 1993.
8. Ogden R W, "Large deformation isotropic elasticity – on the correlation of theory and experiment for incompressible rubberlike solids", Proc. R. Soc. Lond. A. 326, 1972.
9. Treloar L R G, The Physics of Rubber Elasticity, Second Edition, Oxford University Press, 1958.
10. Johnson A R, Quigley C J and Mead J L, "Large strain viscoelastic constitutive models for rubber, Part I: Formulations", Rubber Chemistry and Technology, vol 67, 1994.
11. Johnson A R, Mead J L and Quigley C J, "Large strain viscoelastic constitutive models for rubber, Part II: Determination of material constants", Rubber Chemistry and Technology, vol 68, 1995.
12. ABAQUS/Standard User and Theory Manuals, version 5.8, HKS Inc, USA, 1998.
13. Allport J M and Day A J, "Statistical mechanics material model for the constitutive modelling of elastomeric compounds", Proc. Instn. Mech. Engrs. Volume 10, 1996.
14. Charlton D J, Yang J and Teh K K, "A review of methods to characterise rubber elastic behaviour for use in finite element analysis", Rubber Chemistry and Technology, Vol. 67, 1994.
15. Pascal J, Darque-Ceretti E, Felder E and Pouchelon A, "Rubber-like adhesive in simple shear: stress analysis and fracture morphology of a single lap joint", J. Adhesion Sci. Technol., Vol. 8, No. 5, 1994.
16. Harwood J A C and Payne A R, J. Applied Pol. Sci., vol 12, pp889-901, 1968.
17. Kaliske M and Rothert H, "On the Finite Element implementation of rubber-like materials at finite strains" Engineering Computations, Vol. 14, No. 2, 1997.
18. Raos P, "Modelling of elastic behaviour of rubber and its application in FEA", Plastics, Rubber and Composites Processing and Applications, Vol. 19, No. 5, 1993.
19. Crocker L E, Duncan B C, Hughes R G and Urquhart J M, Hyperelastic modeling of flexible adhesives, CMMT(A)183, May 1999.

20. Duncan B, Crocker L and Urquhart J, Evaluation of hyperelastic Finite Element models for flexible adhesive joints, CMMT(A)285, 2000.
21. Duncan B and Tomlins P, Measurement of strain in bulk adhesive testpieces, NPL Report DMM(B)398, 1994.
22. Dean G, Duncan B, Adams R, Thomas R and Vaughn L, Comparison of bulk and joint specimen tests for determining the shear properties of adhesives, NPL Report CMMT(B)51, 1996.
23. Duncan B, Girardi M and Read B, The preparation of bulk adhesive samples for mechanical testing, NPL Report DMM(B)339, 1994.
24. ISO 15166: 1998 Adhesives – Methods for preparing bulk specimens. Part 1: Two-part systems, International Standards Organisation, 1998.
25. ISO 15166: 1998 Adhesives – Methods for preparing bulk specimens. Part 2: Elevated-temperature curing, one-part systems, International Standards Organisation, 1998.
26. Duncan B, Preparation of bulk adhesive test specimens, CMMT(MN)057, 1999.
27. Olusanya A, Experimental methods for the assessment of the cure of an adhesive, Proceedings of EURADH'96, Institute of Materials, 1996.
28. Olusanya A, A comparison of techniques to assess the cure of adhesives, NPL Report CMMT(B)104, 1996.
29. Mulligan D, Gnaniah S and Sims G, Thermal Analysis Techniques for Composites and Adhesives, NPL Good Practice Guide No 32, 2000.
30. Charalambides M and Olusanya A, The constitutive models suitable for adhesives in some Finite Element codes and suggested methods of generating the appropriate materials data, CMMT(B)131, April 1997.
31. Duncan B, Hyperelastic properties of a polyurethane adhesive, MATC(A)23, 2001.
32. Maxwell A and Duncan B, Evaluation of a multi-functional adhesives test station, CMMT(A)177, April 1999.
33. Duncan B, Maxwell A, Crocker L and Hunt R, Verification of hyperelastic test methods, CMMT(A)226, October 1999.
34. Duncan B, Test methods for determining hyperelastic properties of flexible adhesives, CMMT(MN)054, 1999.
35. ISO 527-2: 1993 Plastics – Determination of tensile properties – Part 2: Test conditions for moulding and extrusion plastics, International Standards Organisation, 1993.
36. ASTM D638-99.
37. ISO 37:1994 Rubber, vulcanised or thermoplastic – Determination of tensile stress-strain properties, International Standards Organisation, 1994.
38. ASTM D412-98 Standard test methods for vulcanised rubber or thermoplastic elastomers – Tension.
39. ISO 3167: 1993, Plastics – Multipurpose test specimens, International Standards Organisation, 1993.

40. Duncan B, Methods for measuring strains at high rates, CMMT(A)133 November 1998.
41. Tomlins P, Yazici M and Dean G, On the determination of stress-strain curves under biaxial loading conditions, NPL Report CMMT(A)298, 2000.
42. Hartmann B, 'Determination of elastic and mechanical properties' Physical Methods of Chemistry, 2nd edition, Volume VII, Eds B.W. Rossiter, R.C. Baetzold, 1991, pp 267-285.
43. Peng S H, Shimbori T and Naderi A, 'Measurement of elastomer's bulk modulus by means of a confined compression test', Presented at the 145th meeting of the Rubber Division, American Chemical Society, Chicago, Illinois, April 1994.
44. Crocker L and Duncan B, Measurement methods for obtaining volumetric coefficients for hyperelastic modeling of flexible adhesives, CMMT(A)286, 2001.
45. Tomlins P E, Measurement and analysis of creep in plastics, NPL Good Practice Guide No 2, 1996.
46. Duncan B C and Ogilvie-Robb K, Creep of flexible adhesive joints, CMMT(A)225, September 1999.
47. Duncan B C and Maxwell A S, Measurement methods for time-dependent properties of flexible adhesives, CMMT(A)178, May 1999.
48. Hu F and Olusanya A, Measurement of creep and stress relaxation in rubber and rubber type materials, CMMT(B)158, December 1997.
49. Duncan B, Crocker L, Urquhart J, Arranz E, Mera R and Broughton W, Failure of flexible adhesive joints, NPL Report MATC(A)34, 2001.
50. Broughton W, Arranz E, Mera R and Duncan B, Size effects on the performance of flexible adhesive joints, Measurement Note MATC(MN)11, 2001.
51. Broughton W and Hinopoulos G, "Evaluation of the single-lap joint using Finite Element Analysis", NPL Report CMMT(A)206, 1999.
52. BS EN 1465:1995, "Adhesives - Determination of tensile lap-shear strength of rigid-to-rigid bonded assemblies".
53. BS EN ISO 9664:1995, "Adhesives - Test methods for fatigue properties of structural adhesives in tensile shear".
54. Broughton W, Hinopoulos G and Mera R, Cyclic fatigue testing of adhesive joints, test method assessment, CMMT(A)191, 1999.
55. ASTM D 1876. Standard test method for peel resistance of adhesives (T-peel test), Volume 15.06, ASTM Standards, 1995, 105-107.
56. ISO 11339: 1993. Adhesives - 180° Peel test for flexible-to-flexible bonded assemblies (T-peel test).

Appendix I

Hyperelastic Models

Commercial FE packages have a large library of hyperelastic models designed for rubber materials. For instance in the HKS package ABAQUS [12] the following models are available: Polynomial; Mooney-Rivlin; reduced polynomial; neo-Hookean; Yeoh; Arruda-Boyce; Ogden and Van der Waals. The Mooney-Rivlin and reduced polynomial are particular cases of the polynomial model, while the neo-Hookean and Yeoh models are special forms of the reduced polynomial model. The Mooney-Rivlin is the most commonly used hyperelastic model.

The hyperelastic material models are described in terms of a strain energy potential, formulated as a function of the strain invariants [12], relating stresses to strains. The majority of these models are phenomenological, meaning the derived constants bear no relationship to the physical or chemical characteristics of rubbers. They consider the bulk properties of the material and attempt to describe the material as an amorphous, isotropic solid; as a result the models can become inaccurate if the material changes state during deformation. Hence, these models are best suited to application such as gum rubber where the effects of such changes are negligible [13].

Polynomial Models

The form of the **polynomial** strain energy potential is:

$$U = \sum_{i+j=1}^N C_{ij} (\bar{I}_1 - 3)^i (\bar{I}_2 - 3)^j + \sum_{i=1}^N \frac{1}{D_i} (J^{el} - 1)^{2i} \quad (I.1)$$

where U is the strain energy potential per reference volume, N is the polynomial order, C_{ij} and D_i are temperature-dependent material parameters, \bar{I}_1 and \bar{I}_2 are the first and second deviatoric strain invariants, defined as:

$$\bar{I}_1 = \overline{\lambda_1^2} + \overline{\lambda_2^2} + \overline{\lambda_3^2} \quad \bar{I}_2 = \overline{\lambda_1^{-2}} + \overline{\lambda_2^{-2}} + \overline{\lambda_3^{-2}} \quad (I.2)$$

where the deviatoric stretches $\overline{\lambda_i} = J^{-1/3} \lambda_i$; λ_i are the principal stretches, J is the total volume ratio, J^{el} is the elastic volume ratio. The D_i parameters allow for the inclusion of compressibility.

The **Mooney-Rivlin** case is obtained from the polynomial form of the hyperelastic model by setting the parameter N to one, i.e. the first order polynomial. The Mooney-Rivlin model uses only linear functions of the invariants.

$$U = C_{10} (\bar{I}_1 - 3) + C_{01} (\bar{I}_2 - 3) + \frac{1}{D_1} (J^{el} - 1)^2 \quad (I.3)$$

The Mooney-Rivlin model is known to be a simple representation of rubbers, though this simplicity also makes it convenient to use. However, it has limited accuracy – it is not a self-

consistent basis for the interpretation of all types of strain [13-15]. Treloar [9] notes that for a single strain type, experiments usually conform to the two term Mooney-Rivlin equation but that using this equation for general strain i.e. a loading type that does not conform to the test, is an unwarranted extrapolation.

The derivation of phenomenological models such as the Mooney-Rivlin is difficult because of the amount of experimental data required to obtain the model coefficients. To improve the accuracy of predictions, it is best to use data from a range of deformation states, especially when trying to predict the behaviour of a material under general loading conditions. ABAQUS suggests data are obtained from uniaxial tension, equibiaxial tension and planar tension. Volumetric data can also be incorporated if compressibility is important [12]. If data from only one state of strain are available, Charlton *et al* [14] make the general recommendation to use the N=1 two term form of the Mooney-Rivlin model. The C_{ij} coefficients required for both the Mooney-Rivlin model and other forms of the polynomial model should really be considered as merely regression coefficients rather than attempt to give them any physical meaning [14], such as relating them to moduli i.e. $E = 6(C_{10} + C_{01}) \approx 3G$ for a Mooney-Rivlin analysis.

In the **Reduced Polynomial** form, the dependence on the second deviatoric strain invariant is suppressed. The model includes only the first strain invariant, this is equivalent to the polynomial form with $C_{ij} = 0$ for $j \neq 0$.

$$U = \sum_{i=1}^N C_{i0} (\bar{I}_1 - 3)^i + \sum_{i=1}^N \frac{1}{D_i} (J^{el} - 1)^{2i} \quad (I.4)$$

The **Neo-Hookean** form is obtained from the reduced polynomial strain energy potential, setting N=1:

$$U = C_{10} (\bar{I}_1 - 3) + \frac{1}{D_1} (J^{el} - 1)^2 \quad (I.5)$$

The Neo-Hookean model has some theoretical relevance since the mathematical representation is analogous to that of an ideal gas: the neo-Hookean potential represents the Helmholtz free energy of a molecular network with Gaussian chain-length distribution.

The **Yeoh** model is obtained from the reduced polynomial form by setting N=3.

$$U = C_{10} (\bar{I}_1 - 3) + C_{20} (\bar{I}_1 - 3)^2 + C_{30} (\bar{I}_1 - 3)^3 + \frac{1}{D_1} (J^{el} - 1)^2 + \frac{1}{D_2} (J^{el} - 1)^4 + \frac{1}{D_3} (J^{el} - 1)^6 \quad (I.6)$$

In all the above equations, the parameters are the same as those defined above for the polynomial model.

Ogden Model

The **Ogden** strain energy potential is expressed in terms of principal stretches. In ABAQUS the form of the Ogden strain energy potential is

$$U = \sum_{i=1}^N \frac{2\mu_i}{\alpha_i^2} (\bar{\lambda}_1^{\alpha_i} + \bar{\lambda}_2^{\alpha_i} + \bar{\lambda}_3^{\alpha_i} - 3) + \sum_{i=1}^N \frac{1}{D_i} (J^{el} - 1)^{2i} \quad (I.7)$$

where $\bar{\lambda}_i$ are the deviatoric principal stretches. N is the order of the polynomial, μ_i , α_i , and D_i are temperature-dependent material properties. The Mooney-Rivlin and neo-Hookean forms of polynomial model can also be obtained from the general Ogden strain energy potential for special choices of μ_i and α_i .

The Ogden model is also a phenomenological model that makes no attempt to link the adjustable parameters to any physical deformation model. The model generally requires more than one set of experimental data to obtain the number of constants required to capture the state of deformation dependence. The Ogden function has the advantage that the exponent values (α_i) can be any real number, which gives the model the ability to fit non-linear material test data [14].

Van der Waals Model

The form of the **Van der Waals** strain energy potential is

$$U = \mu \left\{ -(\lambda_m^2 - 3) [\ln(1 - \eta) + \eta] - \frac{2}{3} a \left(\frac{\tilde{I} - 3}{2} \right)^{\frac{3}{2}} \right\} + \frac{1}{D} \left(\frac{J_{el}^2 - 1}{2} - \ln J_{el} \right) \quad (I.8)$$

where $\tilde{I} = (1 - \beta)\bar{I}_1 + \beta\bar{I}_2$ and $\eta = \sqrt{\frac{\tilde{I} - 3}{\lambda_m^2 - 3}}$

Here, U is the strain energy per unit of reference volume; μ is the initial shear modulus; λ_m is the locking stretch; a is the global interaction parameter; β is an invariant mixture parameter and D governs compressibility. These parameters can be temperature dependent. \bar{I}_1 and \bar{I}_2 are the first and second deviatoric strain invariants, as above; J is the total volume ratio and J^{el} is the elastic volume ratio. The Van Der Waals model is sometimes known as the Killian model.

The Van der Waals strain energy potential is analogous to the equations of state of a real gas. This introduces two additional material parameters, the locking stretch (λ_m), which accounts for the finite extendibility of the non-Gaussian chain network, and the global interaction parameter (a), which models the interaction between chains.

Arruda-Boyce Model

The **Arruda-Boyce** model has a strain energy potential of the form

$$U = \mu \left\{ \frac{1}{2} (\bar{I}_1 - 3) + \frac{1}{20\lambda_m^2} (\bar{I}_1^2 - 9) + \frac{11}{1050\lambda_m^4} (\bar{I}_1^3 - 27) + \frac{19}{7000\lambda_m^6} (\bar{I}_1^4 - 81) + \frac{519}{673750\lambda_m^8} (\bar{I}_1^5 - 243) + \dots \right\} + \frac{1}{D} \left(\frac{J_{el}^2 - 1}{2} - \ln J_{el} \right) \quad (I.9)$$

where U is the strain energy per unit of reference volume; μ , λ_m and D are temperature dependent material parameters, \bar{I}_1 is the first deviatoric strain invariant, J_{el} is the elastic volume ratio; and λ_i are the principal stretches.

The Arruda-Boyce model is a constitutive relationship for nonlinear elasticity, which should better describe the state of deformation dependant response of rubber materials. The aim of the model is to represent the behaviour of the material while requiring only a small number of “physically based” parameters [7]. This model is also known as the eight-chain model since it was developed from a representative volume element where eight springs emanate from the centre of a cube to its corners. The Arruda-Boyce strain energy potential depends on the first strain invariant only. The physical interpretation of this is that the eight chains are stretched equally under the action of a general deformation state.

When making predictions using any of these models, the stability of the model is of great importance. To obtain stability the requirement is for the energy function to obey the laws of thermodynamics i.e. energy functions that mathematically require the solid to increase its internal energy when work is done on it [10]. The material constants are only regression coefficients. They accurately fit experimental data, but this does not assure thermodynamic stability. If stability is not considered while selecting material constants, the numerical procedures may have difficulty converging or giving meaningful results. ABAQUS performs stability checks and warns of unstable ranges and types of deformation. Unstable models may have difficulty converging to a solution during FEA. A constrained regression analysis can be used for the selection of material constants, as demonstrated by Johnson *et al* [11]. In this case, when the regression analysis is performed on the experimental data, the analysis is constrained using numerical algorithms, which select only positive material constants to fit the experimental data. Although the resulting model does not fit the experimental data as accurately as one based on an unconstrained regression analysis, it should be more thermodynamically stable.

For some models, stability is assured by following some simple rules [12].

- For positive values of initial shear modulus, μ , and locking stretch, λ_m , the Arruda-Boyce form is always stable.
- For positive values of the coefficients C_{10} the neo-Hookean form is always stable.
- Given positive values of the initial shear modulus, μ , and locking stretch, λ_m , the stability of the Van der Waals model depends on the global interaction parameter, a .
- For the Yeoh model, stability is assured if all $C_{i0} > 0$. Typically, however, C_{20} will be negative. Thus, reducing the absolute value of C_{20} or magnifying the absolute value of C_{10} will help make the Yeoh model more stable.

The FE predictions made using hyperelastic models have frequently been compared with experimental data obtained by Treloar [6]. Treloar tested vulcanised rubber in simple tension, pure shear (planar tension) and uniform equibiaxial tension. All samples were cut from the same sheet to avoid batch-to-batch variation, which is common in rubbers. For example, Treloar's data was compared to predictions made using the Ogden model, and the predictions were found to be in good agreement [8]. Arruda and Boyce [7] also showed good agreement between Treloar's data and predictions obtained using the Arruda-Boyce model. The ABAQUS manuals also use the Treloar data to illustrate the fits provided by the various hyperelastic models.

Arruda and Boyce [7] also repeated their work with three other materials (silicon, gum and neoprene rubber) with reasonable results. Allport and Day [13] tested tensile compression blocks of styrene-butadiene (SBR). Their work indicated that the Arruda-Boyce model could give good agreement with measured behaviour in both tension and compression. The authors suggested that this was a considerable advance over the Mooney-Rivlin and Ogden type models, which require different coefficients in tension and compression. Comparisons with Mooney-Rivlin and Ogden models demonstrated that good agreement was possible by tuning coefficients. Kaliske and Rothert [17] compared experimental results from rubber samples in a non-homogeneous shear test with predictions from selected hyperelastic models. The authors found that the Yeoh and Arruda-Boyce models gave the best fits followed by the Van der Waals model.

Raos [18] compared the prediction from four models (neo-Hookean, Mooney-Rivlin, Van der Waals and Ogden) with experimental tests carried out on an SBR rubber compound under conditions of uniaxial and biaxial loads. In particular, the author investigated the influence of the initial strain ranges used to obtain the coefficients, while predictions were made over the full strain range. It was found that even if the strain range is chosen adequately, the neo-Hookean and Mooney-Rivlin models could describe experimental data only in compression and moderate extension (up to 80%). The Van der Waals and Ogden models covered the whole range of applied strains with acceptable results, though these models exhibited some instability and sensitivity to the change of strain range. Also, it was found that the biaxial tests were very sensitive and required reliable maintenance of testing boundary conditions. Of the four models, the Van der Waals and Ogden models were especially sensitive to biaxial conditions.

Briefly summarised, the Mooney-Rivlin model is the most commonly used model, its simplicity making it convenient to use, although, if predicting the behaviour of a rubber under general loading conditions it is best to use experimental data from a range of experimental tests (uniaxial, biaxial and planar tension). The Arruda-Boyce, neo-Hookean and Van der Waals models offer a physical interpretation and provide a better description of general deformation modes when the parameters are based only on one test. In all cases, it is best to obtain experimental data over the range of strain of interest (this is especially true of the Ogden and polynomial models), and to select the model coefficients carefully to ensure stability. In the literature reviewed above, hyperelastic models have been used to predict the behaviour of ideal rubbers. No reference is made to correlations between predictions and experiment for non-idealised materials, e.g. filled rubbers or blends.

REFERENCES *Please refer to main references section*

Appendix II

Example sets of experimental data

(a) Uniaxial tension data

The data set is laid out as nominal stress, nominal strain.

```
0, 0
0.271555467, 0.025
0.549467814, 0.05
0.812604312, 0.075
1.053771927, 0.1
1.280233907, 0.125
1.485743741, 0.15
1.689128765, 0.175
1.864706226, 0.2
2.030635194, 0.225
2.188082036, 0.25
2.333341099, 0.275
2.452510949, 0.3
2.566165619, 0.325
2.674112967, 0.35
2.761621673, 0.375
2.828238548, 0.4
2.902696602, 0.425
2.948654277, 0.45
3.004963168, 0.475
3.028566578, 0.5
```

(b) Volumetric tension data

This data set is laid out as pressure (stress), 1/volume ratio (see Section 6.1.2)

```
0, 1
0.45442474, 0.996160902
0.829431389, 0.990139817
1.19942655, 0.985288402
1.511617225, 0.979632977
1.804518656, 0.974337796
2.078505554, 0.968581429
2.332030849, 0.962321388
2.568763456, 0.955791812
2.776213328, 0.949984713
2.982650174, 0.942455596
3.155916398, 0.935514361
3.314711473, 0.928250844
3.457449226, 0.920949825
3.588719612, 0.914356841
3.693092286, 0.906551517
3.799212658, 0.898723965
3.856359792, 0.890674342
3.941831572, 0.883205674
4.01287856, 0.875054806
```

(c) Stress Relaxation Data

The material definition needs to contain both elastic or hyperelastic and visco-elastic properties, for example:

```
*MATERIAL,NAME=RUBBER
*ELASTIC
2500.0, 0.35
*VISCOELASTIC, TIME=RELAXATION TEST DATA, ERRTOL=0.05
*INCLUDE,INPUT=visc_rel.dat(if including from a data file)
** for direct entry or format for *visc_rel.dat
```

data are laid out normalised relaxation, time

```
*SHEAR TEST DATA
```

```
0.4363, 0.2
0.3462, 0.58
0.3252, 0.68
0.2995, 0.84
0.2988, 0.86
0.2785, 1.02
0.2521, 1.32
0.2396, 1.5
0.2248, 1.8
0.2163, 2
0.1929, 2.6
0.1813, 3.02
0.1758, 3.4
0.1603, 4.1
0.1548, 4.6
0.1502, 5.08
0.1463, 5.3
0.1362, 6.3
0.1323, 6.9
0.1206, 8.96
0.1167, 9.86
0.1136, 10
0.0886, 20
0.0584, 60
0.0509, 90
0.0394, 190
0.0375, 230
0.0356, 270
0.0333, 340
0.0232, 1920
0.0210, 3801.76
0.0195, 5098.68
0.0192, 6120
0.0179, 7849.98
0.0171, 10970.78
0.0163, 14531.18
0.0156, 15764.06
```

(d) Creep Material Definition

The material definition needs to contain both elastic or hyperelastic and visco-elastic properties, for example:

```
*MATERIAL, NAME=MAT3
*HYPERELASTIC
0.557363,-0.099368,0,20.
*VISCOELASTIC, TIME=CREEP TEST DATA, ERRTOL=0.02
****INCLUDE, INPUT=visc_cr.dat (if including from a data file)
** for direct entry or format for *visc_cr.dat
```

data are laid out normalised creep strain, time

```
*SHEAR TEST DATA
```

```
1.058578975, 1
1.087868463, 2
1.125504048, 3
1.150604858, 4
1.16735957, 5
1.175705667, 6
1.192460379, 7
1.209183833, 8
1.221749867, 9
1.305429652, 19
1.355631271, 29
1.393298115, 39
1.426776281, 49
1.472789222, 69
1.518802163, 89
1.531368197, 109
1.581569817, 149
1.615047982, 189
1.66943828, 259
1.694539089, 316
1.81169704, 616
1.899565503, 1016
1.9539558, 1416
2.05017036, 2516
2.125504048, 3586
2.209183833, 5586
2.271920228, 7586
2.330499203, 9586
2.4309337, 15586
2.481135319, 20586
2.569003782, 30586
2.610828045, 36286
2.677784377, 46286
2.707073865, 56286
2.815854459, 76286
2.866056078, 96286
2.882810791, 106286
2.979025351, 156286
3.041793004, 206286
3.087805945, 256286
3.158950955, 326286
```

Appendix III

Coefficient calculation input file

```

** FILE NAME: "coefcalc.inp"
*HEADING
  HYPERELASTIC TEST DATA FITTING
**
*RESTART,WRITE,FREQUENCY=1
**
*****
** NODE & ELEMENT DEFINITION **
*****
*NODE,NSET=ALL
1,
2,1.
3,1.,1.,
4,0.,1.,
5,0.,0.,1.
6,1.,0.,1.
7,1.,1.,1.
8,0.,1.,1.
*NSET,NSET=FACE1
1,2,3,4
*NSET,NSET=FACE2
5,6,7,8
*NSET,NSET=FACE3
1,2,5,6
*NSET,NSET=FACE4
2
*NSET,NSET=FACE42
3,6,7
*NSET,NSET=FACE5
3,4,7,8
*NSET,NSET=FACE6
4,1,8,5
*EQUATION
2
FACE42,1,1, 2,1,-1
**
*ELEMENT,TYPE=C3D8RH,ELSET=ONE
1,1,2,3,4,5,6,7,8
*SOLID SECTION,ELSET=ONE,MATERIAL=TREL
*MATERIAL,NAME=TREL
**
*****
** MODEL DEFINITIONS **
*****
** -----
**   Polynomial model (N = 1 OR 2)
**
** *HYPERELASTIC, POLYNOMIAL, N=1, TEST DATA INPUT
** -----
**   Mooney-Rivlin model
** *HYPERELASTIC, MOONEY-RIVLIN, TEST DATA INPUT
** this is equivalent to
** *HYPERELASTIC, POLYNOMIAL, N=1, TEST DATA INPUT
** -----
**   Reduced Polynomial model (1≤N≤6)
** *HYPERELASTIC,REDUCEDPOLYNOMIAL,N=2,TEST DATA INPUT
** -----
**   Neo-Hookean model
** *HYPERELASTIC,NEO HOOKE,TEST DATA INPUT
** this is equivalent to
** *HYPERELASTIC,REDUCEDPOLYNOMIAL,N=1,TEST DATA INPUT

```

```
** -----
**      Yeoh model
** *HYPERELASTIC,YEOH HOOKE,TEST DATA INPUT
** this is equivalent to
** *HYPERELASTIC,REDUCEDPOLYNOMIAL,N=3,TEST DATA INPUT
** -----
**      Ogden model              (1≤N≤6)
** *HYPERELASTIC,OGDEN,N=3,TEST DATA INPUT
** -----
**      Van der Waals model
** *HYPERELASTIC,VAN DER WAALS,TEST DATA INPUT
** -----
**      Arruda-Boyce model
** *HYPERELASTIC,ARRUDA-BOYCE,TEST DATA INPUT
** -----
*****
** INPUTTING TEST DATA **
*****
*UNIAXIAL TEST DATA
*INCLUDE,INPUT=uniaxial.dat
*BIAXIAL TEST DATA
* INCLUDE,INPUT =biaxial.dat
*PLANAR TEST DATA
* INCLUDE,INPUT =planar.dat
*VOLUMETRIC TEST DATA
*INCLUDE, INPUT=volumetric.dat
*****
** ANALYSIS STEP **
*****
*STEP,NLGEOM, INC=50
*STATIC,DIRECT
0.02, 0.48
*BOUNDARY,OP=NEW
FACE1,3
FACE3,2
FACE6,1
FACE4,1,1,0.48
*ENERGY PRINT
*EL PRINT,FREQUENCY=5
S
E
*NODE PRINT,FREQUENCY=5
U,RF
*NODE FILE,FREQUENCY=1
U,RF
*EL FILE,FREQUENCY=1
S,E,ENER,LE,NE
*END STEP
```

Appendix IV

Single element analysis input file

```

** FILE NAME: "singelem.inp"
*HEADING
  SINGLE ELEMENT ANALYSIS
*RESTART,WRITE,FREQUENCY=1
*NODE,NSET=ALL
1,
2,1.
3,1.,1.,
4,0.,1.,
5,0.,0.,1.
6,1.,0.,1.
7,1.,1.,1.
8,0.,1.,1.
*NSET,NSET=FACE1
1,2,3,4
*NSET,NSET=FACE2
5,6,7,8
*NSET,NSET=FACE3
1,2,5,6
*NSET,NSET=FACE4
2
*NSET,NSET=FACE42
3,6,7
*NSET,NSET=FACE5
3,4,7,8
*NSET,NSET=FACE6
4,1,8,5
**
** Since the S11 output is Cauchy or true stress,
** we need to determine the nominal
** stress for post-processing.
** Nodes 3,6,7 are tied to node 2 in dof 1 so that:
** Nominal stress (dof 1) = RF1 (@ node 2) /
** Original area (w/c is 1 x 1 = 1)
**
*EQUATION
2
FACE42,1,1, 2,1,-1
*ELEMENT,TYPE=C3D8RH,ELSET=ONE
1,1,2,3,4,5,6,7,8
*SOLID SECTION,ELSET=ONE,MATERIAL=TREL
*MATERIAL,NAME=TREL
**
*HYPERELASTIC,MOONEY-RIVLIN
0.140135, 2.01861, 0.03830735
**
*STEP,NLGEOM, INC=50
Step 1: Uniaxial Tension
*STATIC,DIRECT
0.02, 0.48
*BOUNDARY,OP=NEW
FACE1,3
FACE3,2
FACE6,1
FACE4,1,1,0.48
*ENERGY PRINT
*EL PRINT,FREQUENCY=5
S
E
*NODE PRINT,FREQUENCY=5

```

```
U,RF
*NODE FILE,FREQUENCY=1
U,RF
*EL FILE,FREQUENCY=1
S,E,ENER,LE,NE
*END STEP
*STEP,NLGEOM,INC=50
Step 2: Unload
*STATIC,DIRECT
0.01,0.1
*BOUNDARY,OP=MOD
FACE4,1,1,0.
*END STEP
*STEP,NLGEOM,INC=50
Step 3: Biaxial Tension
*STATIC,DIRECT
0.01,0.2
*BOUNDARY,OP=NEW
FACE1,3
FACE3,2
FACE6,1
FACE4,1,1,0.2
FACE5,2,2,0.2
*END STEP
*STEP,NLGEOM,INC=50
Step 4: Unload
*STATIC,DIRECT
0.01,0.1
*BOUNDARY,OP=MOD
FACE4,1
FACE5,2
*END STEP
*STEP,NLGEOM,INC=50
Step 5: Planar Tension
*STATIC,DIRECT
0.01,0.2
*BOUNDARY,OP=NEW
FACE1,3
FACE3,2
FACE5,2
FACE6,1
FACE4,1,1,0.2
*END STEP
```

Appendix V

ABAQUS Element Types

The elements used in the lap joint mesh were solid (continuum) elements. The solid elements in ABAQUS are suitable for linear analysis and also for complex nonlinear analyses involving plasticity and large deformations. There are a number of continuum elements available within the ABAQUS element library [12]. A brief description of the attributes of the elements used for the lap joint analysis is given below and summarised in Table V.1.

Quadrilateral elements were chosen over triangular elements as the quadrilateral elements have a better convergence rate and sensitivity to mesh orientation in regular meshes is not an issue. Quadrilateral elements perform best if their shape is approximately rectangular. The elements become much less accurate when they are initially distorted.

The second order form of the quadrilateral elements was used because they provide higher accuracy than first order elements for ‘smooth’ problems that do not involve complex contact conditions or impact. Second order elements have more nodes per element than first order elements i.e. have a midside node. They capture stress concentrations more effectively and are better for modelling geometric features.

Reduced integration is available for quadratic elements and was utilised in the lap joint analysis. It uses a lower-order integration to form the element stiffness. Reduced integration reduced the running time of an analysis. Second order reduced integration elements generally yield more accurate results than the corresponding fully integrated elements.

A further element option is the hybrid element. Hybrid elements are intended mainly for use with incompressible and almost incompressible materials. For a near incompressible material, a very small change in displacement produces extremely large changes in pressure. Therefore, a purely displacement-based solution is too sensitive to be useful numerically. This singular behaviour is removed by treating the pressure stress as an independently interpolated basic solution variable, coupled to the displacement. This independent interpolation of pressure stress is the basis of the hybrid elements. Hybrid elements have more internal variables than non-hybrid elements, which increases running time. Hybrid elements are recommended for hyperelastic materials.

For structural applications, the ABAQUS element library includes plane stress, plane strain and generalised plane strain elements. Plane stress elements can be used when the thickness of a body is small relative to its lateral (in-plane) dimensions. This element is generally used for thin, flat bodies. In contrast, plane strain elements are generally used for modelling bodies that are very thick relative to their lateral dimensions. In these elements it is assumed that the strains in the loaded body are functions of the planar coordinates only and out-of-plane normal and shear strains are equal to zero. An alternative type of plane strain element is the generalised plane strain element. In this case, the formulation used places the model between two rigid planes that can only move closer or further apart, thus a lap joint mesh would have the ability to respond to Poisson’s contractions. It is assumed that the deformation of the model is independent of the axial position so the relative motion of the two planes causes a direct strain in the axial direction only. There are no transverse shear strains. Both plane strain and generalised plane strain elements have been considered in the analysis of the lap joint.

Table V.1 Attributes of the solid elements chosen for modelling flexible adhesives using hyperelastic material models

Element Type	Uses/Advantages	Disadvantages
Plane strain	For bodies that are thick relative to its lateral (in-plane) dimension	Assume out-of-plane normal and shear strains are zero
Generalised plane strain	For bodies that are thick relative to its lateral (in-plane) dimension Have ability to allow to Poisson's contraction	
Quadratic	Better convergence than triangular elements Perform best if initial shape is approximately rectangular	Much less accurate if initially distorted
2 nd order quads	Higher accuracy than 1 st order quads for 'smooth' problems Capture stress concentrations more effectively than 1 st order Better for modelling geometric features	Avoid using for contact/impact problems
Reduced integration	Reduced running time of analysis 2 nd order reduced integration elements generally yield more accurate results than fully integrated 2 nd order elements	
Hybrid	Intended mainly for use with incompressible and almost incompressible materials Recommended when using hyperelastic materials	Increased running time